
Composite Flow Matching for Reinforcement Learning with Shifted-Dynamics Data

Lingkai Kong* Haichuan Wang* Tonghan Wang Guojun Xiong Milind Tambe
Department of Computer Science
Harvard University

Abstract

Incorporating pre-collected offline data from a source environment can significantly improve the sample efficiency of reinforcement learning (RL), but this benefit is often challenged by discrepancies between the transition dynamics of the source and target environments. Existing methods typically address this issue by penalizing or filtering out source transitions in high dynamics-gap regions. However, their estimation of the dynamics gap often relies on KL divergence or mutual information, which can be ill-defined when the source and target dynamics have disjoint support. To overcome these limitations, we propose COMPFLOW, a method grounded in the theoretical connection between flow matching and optimal transport. Specifically, we model the target dynamics as a conditional flow built upon the output distribution of the source-domain flow, rather than learning it directly from a Gaussian prior. This composite structure offers two key advantages: (1) improved generalization for learning target dynamics, and (2) a principled estimation of the dynamics gap via the Wasserstein distance between source and target transitions. Leveraging our principled estimation of the dynamics gap, we further introduce an optimistic active data collection strategy that prioritizes exploration in regions of high dynamics gap, and theoretically prove that it reduces the performance disparity with the optimal policy. Empirically, COMPFLOW outperforms strong baselines across several RL benchmarks with shifted dynamics.

1 Introduction

Reinforcement Learning (RL) has demonstrated the ability to train policies capable of achieving remarkable performance across a diverse range of complex sequential decision-making tasks [47, 49]. However, in many real-world applications, such as robotics [25, 54], healthcare [63], or wildlife conservation [60, 61, 26], the opportunity for extensive interactions with the environment is either prohibitively expensive, unsafe, or simply unavailable, thereby hindering efficient policy learning. To address this issue and enhance sample efficiency during online training, one promising approach involves merging a pre-collected, static offline dataset [53, 39]. This allows the agent to learn from a richer set of experiences, potentially accelerating convergence and improving initial performance.

A critical challenge in RL with using offline data arises when the dataset is collected from source environments whose dynamics differ from those of the target domain, where the agent is simultaneously interacting and learning [44]. This issue, commonly referred to as *shifted dynamics*, can introduce severe mismatches that bias policy updates, destabilize the learning process, and ultimately degrade performance. For instance, in the conservation domain, historical data collected from one national park may not transfer well to another, as geography and poacher behavior can vary significantly across regions [60]. In robotics, differences in physical parameters such as friction can result in transition dynamics that diverge from the source domain.

*Equal contribution. Corresponding author: lingkaikong@g.harvard.edu

To address these challenges, existing methods either penalize the rewards or value estimates of source transitions with high dynamics gap [41, 32], or filter out such transitions entirely [58]. However, these approaches face key limitations. Most notably, the estimation of the dynamics gap typically relies on KL divergence or mutual information, both of which can be ill-defined when the source and target transition dynamics have disjoint support [2, 43].

In this paper, we propose COMPFLOW, a novel method for RL with shifted-dynamics data by leveraging the theoretical connection between flow matching and optimal transport. Specifically, we model the transition dynamics of the target domain using a composite flow architecture, where the target flow is constructed on top of the output distribution of the source flow, rather than being learned from a Gaussian prior. This design enables a principled estimation of the dynamics gap via the Wasserstein distance between the source and target transition distributions. On the theoretical side, we show that the composite flow formulation reduces generalization error by reusing structural knowledge from the source domain, particularly when target domain data is scarce—outperforming standard approaches that learn the target flow from scratch.

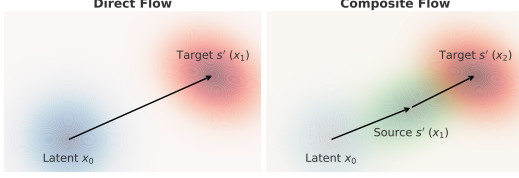


Figure 1: Comparison between direct and composite flow matching. Composite flow first transports from a Gaussian latent variable to the source domain distribution, then adapts to the target distribution via optimal transport flow matching.

Building on the dynamics gap estimated by composite flow matching using the Wasserstein distance, we go beyond selectively merging source transitions with low dynamics gap and further propose an active data collection strategy that targets regions exhibiting high dynamics gap relative to the source domain. Such regions are often underrepresented in the replay buffer due to the dominance of low-gap samples. Our theoretical analysis shows that targeted exploration in these high-gap regions can further close the performance gap with respect to the optimal policy.

Our contributions are summarized as follows: (1) We introduce a composite flow model that estimates the dynamics gap by computing the Wasserstein distance between conditional transition distributions. We provide theoretical analysis showing that this approach achieves lower generalization error compared to learning the target dynamics from scratch. (2) Leveraging this principled estimation, we propose a new data collection strategy that encourages the policy to actively explore regions with high dynamics gap. We also provide a theoretical analysis of its performance benefits. (3) We empirically validate our method on various public RL benchmarks with shifted dynamics and demonstrate that COMPFLOW outperforms or matches state-of-the-art baselines across these tasks.

2 Problem Statement and Background

2.1 Problem Definition

We consider two infinite-horizon MDPs: $\mathcal{M}_{\text{src}} := (\mathcal{S}, \mathcal{A}, p_{\text{src}}, r, \gamma)$ and $\mathcal{M}_{\text{tar}} := (\mathcal{S}, \mathcal{A}, p_{\text{tar}}, r, \gamma)$, sharing the same state/action spaces, reward function $r : \mathcal{S} \times \mathcal{A} \rightarrow \mathbb{R}$, and discount factor $\gamma \in (0, 1)$, but differing in transition dynamics:

$$p_{\text{src}}(s'|s, a) \neq p_{\text{tar}}(s'|s, a), \quad \text{for some } (s, a).$$

We assume that the reward signals are bounded, i.e., $|r(s, a)| \leq r_{\text{max}}, \forall s, a$. For any policy π , we define its discounted state-action visitation under MDP \mathcal{M} as $\rho_{\mathcal{M}}^{\pi}(s, a) := (1 - \gamma) \sum_{t=0}^{\infty} \gamma^t P_{\mathcal{M}, t}^{\pi}(s) \pi(a | s)$, and the corresponding state visitation as $d_{\mathcal{M}}^{\pi}(s) := \sum_a \rho_{\mathcal{M}}^{\pi}(s, a)$. The expected return is $\eta_{\mathcal{M}}(\pi) := \mathbb{E}_{(s, a) \sim \rho_{\mathcal{M}}^{\pi}}[r(s, a)]$.

Definition 2.1 (Online Dynamics Adaptation with Offline Data). Given an offline dataset $\mathcal{D}_{\text{src}} = \{(s_i, a_i, s'_i, r_i)\}_{i=1}^N$ from \mathcal{M}_{src} and limited online access to \mathcal{M}_{tar} , the objective is to learn a policy π maximizing $\eta_{\mathcal{M}_{\text{tar}}}(\pi)$, ideally approaching $\eta_{\mathcal{M}_{\text{tar}}}(\pi^*)$, where $\pi^* := \arg \max_{\pi} \eta_{\mathcal{M}_{\text{tar}}}(\pi)$.

Lemma 2.2 (Return Bound between Source Domain and Target Domain [32]). *Let the empirical behavior policy in \mathcal{D}_{src} be $\pi_{\mathcal{D}_{\text{src}}}(a | s)$. Define $C_1 = \frac{2r_{\text{max}}}{(1-\gamma)^2}$. Then for any policy π ,*

$$\begin{aligned} \eta_{\mathcal{M}_{\text{tar}}}(\pi) - \eta_{\mathcal{M}_{\text{src}}}(\pi) &\geq -2C_1 \mathbb{E}_{(s, a) \sim \rho_{\mathcal{M}}^{\pi_{\mathcal{D}_{\text{src}}}}, s' \sim p_{\text{src}}} [D_{\text{TV}}(\pi(\cdot | s') \parallel \pi_{\mathcal{D}_{\text{src}}}(\cdot | s'))] \\ &\quad - C_1 \mathbb{E}_{(s, a) \sim \rho_{\mathcal{M}}^{\pi_{\mathcal{D}_{\text{src}}}}} [D_{\text{TV}}(p_{\text{tar}}(\cdot | s, a) \parallel p_{\text{src}}(\cdot | s, a))]. \end{aligned}$$

This bound highlights two key sources of return gap between domains: (1) the mismatch between the learned policy and the behavior policy in the offline dataset, and (2) the shift in environment dynamics. The former can be mitigated through behavior cloning [32, 59], while the latter can be addressed by filtering out source transitions with large dynamics gaps [58, 34]. A central challenge lies in accurately estimating this gap. Existing methods often rely on KL divergence or mutual information [41, 32], which can be ill-defined when the two dynamics have disjoint support.

2.2 Flow Matching

In this paper, we will adopt flow matching [29, 31, 1] to model transition dynamics in reinforcement learning, owing to its ability to capture complex distributions. Flow Matching (FM) offers a simpler alternative to denoising diffusion models [20, 51], which are typically formulated using stochastic differential equations (SDEs). In contrast, FM is based on deterministic ordinary differential equations (ODEs), providing advantages such as faster inference, and often improved sample quality.

The goal of FM is to learn a time-dependent velocity field $v_\theta(x, t) : \mathbb{R}^d \times [0, 1] \rightarrow \mathbb{R}^d$, parameterized by θ , which defines a flow map $\psi_\theta(x_0, t)$. This map is the solution to the ODE

$$\frac{d}{dt}\psi_\theta(x_0, t) = v_\theta(\psi_\theta(x_0, t), t), \quad \psi_\theta(x_0, 0) = x_0,$$

and transports samples from a simple source distribution $p_0(x)$ (e.g., an isotropic Gaussian) at time $t = 0$ to a target distribution $p_1(x)$ at time $t = 1$. In practice, generating a sample from the target distribution involves drawing $x_0 \sim p_0(x)$ and integrating the learned ODE to obtain $x_1 = \psi_\theta(x_0, 1)$.

A commonly used training objective in flow matching is the *linear path matching loss*

$$\mathcal{L}(\theta) = \mathbb{E}_{t \sim \mathcal{U}[0,1], x_0 \sim p_0(x_0), x_1 \sim p_1(x_1)} \left[\|v_\theta(x_t, t) - (x_1 - x_0)\|_2^2 \right], \quad (1)$$

where $x_t = (1-t)x_0 + tx_1$ denotes the linear interpolation between x_0 and x_1 . Using linear interpolation paths encourages the learned flow to follow nearly straight-line trajectories, which reduces discretization error and improves the computational efficiency of ODE solvers during sampling.

2.3 Optimal Transport Flow Matching and Wasserstein Distance

Optimal Transport Flow Matching (OT-FM) establishes a direct connection between flow-based modeling and Optimal Transport (OT), providing a principled framework for quantifying the discrepancy between two distributions. This connection is especially valuable in our setting, where a key challenge is to measure the distance between two conditional transition distributions.

Let $c : \mathbb{R}^d \times \mathbb{R}^d \rightarrow \mathbb{R}$ be a cost function. Optimal transport aims to find a coupling $q^* \in \Pi(p_0, p_1)$ —a joint distribution with marginals p_0 and p_1 —that minimizes the expected transport cost:

$$\inf_{q \in \Pi(p_0, p_1)} \int c(x_0, x_1) dq(x_0, x_1).$$

This minimum defines the Wasserstein distance $W_c(p_0, p_1)$ between the two distributions under the cost function c . When $c(x_0, x_1) = \|x_0 - x_1\|^2$, the resulting distance is known as the squared 2-Wasserstein distance.

In the training objective of Eq. 1, when sample pairs (x_0, x_1) are drawn from the optimal coupling q^* , the flow model trained with the linear path matching loss learns a vector field that approximates the optimal transport plan. The transport cost of the learned flow is equal to the Wasserstein distance

$$\mathbb{E}_{x_0 \sim p_0} \left[\|\psi_\theta(x_0, 1) - x_0\|_2^2 \right] = W_2^2(p_0, p_1).$$

For theoretical justification, see Theorem 4.2 in [42].

In practice, the optimal coupling π^* is approximated using mini-batches by solving a discrete OT problem between empirical samples from p_0 and p_1 . The use of mini-batch OT has also been shown to implicitly regularize the transport plan [13, 14], as the stochasticity from independently sampled batches induces behavior similar to entropic regularization [9]. Further details of the OT-FM training procedure are provided in Appendix B.

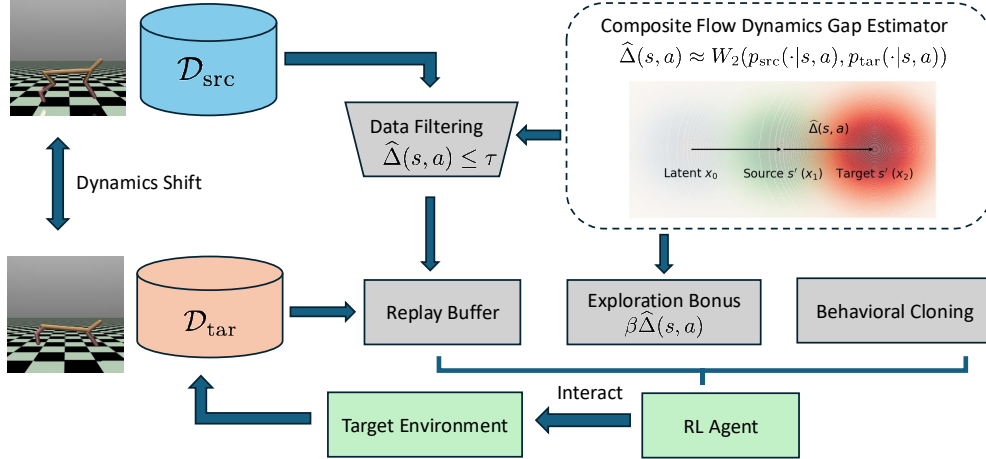


Figure 2: Overall Framework of COMPFLOW. To estimate the dynamics gap, we propose composite flow matching, which computes the Wasserstein distance between source and target conditional transition distributions. Guided by the estimated dynamics gap, we augment policy training with source-domain transitions that exhibit low discrepancy from the target dynamics, and incorporate a behavior cloning objective to stabilize learning. To enhance data diversity and facilitate adaptation, we further encourage exploration in regions with high dynamics gap.

3 Proposed Method

In this section, we introduce our method, COMPFLOW. We begin by presenting a composite flow matching approach to estimate the dynamics gap via Wasserstein distance. Next, we propose a data collection strategy that actively explores high dynamics-gap regions and provide a theoretical analysis of its benefits. Finally, we describe the practical implementation details of our method.

3.1 Estimating Dynamics Gap via Composite Flow

To estimate the dynamics gap, we begin by learning the transition dynamics in both the source and target domains. While flow matching offers a powerful framework for modeling complex transition dynamics, the limited number of training samples in the target domain poses a significant challenge. Naively training separate flow models for each domain can lead to poor generalization in the target domain due to data scarcity.

To mitigate this, we propose a **composite flow** formulation. Instead of learning the target transition model $p_{\text{tar}}(s'|s, a)$ from scratch, we leverage structural knowledge from a well-trained source model $p_{\text{src}}(s'|s, a)$. This enables knowledge transfer across domains while adapting to the specific characteristics of the target environment.

Source Flow. We begin by learning a conditional flow model for the source domain. Let $x_0 \sim \mathcal{N}(0, \mathbf{I})$ be the initial latent variable. The source flow map $\psi_{\theta}^{\text{src}}(x_0, t|s, a)$ is defined as the solution to the following ODE:

$$\frac{d}{dt}\psi_{\theta}^{\text{src}}(x_0, t|s, a) = v_{\theta}^{\text{src}}(\psi_{\theta}^{\text{src}}(x_0, t|s, a), t, s, a), \quad \psi_{\theta}^{\text{src}}(x_0, 0|s, a) = x_0.$$

Solving this ODE from $t = 0$ to 1 produces an intermediate representation: $x_1 = \psi_{\theta}^{\text{src}}(x_0, 1|s, a)$.

Target Flow. Instead of learning a target flow directly from a Gaussian prior, we initialize it from the intermediate representation x_1 produced by the source flow. The target flow map $\psi_{\phi}^{\text{tar}}(x, t|s, a)$ is defined as:

$$\frac{d}{dt}\psi_{\phi}^{\text{tar}}(x, t|s, a) = v_{\phi}^{\text{tar}}(\psi_{\phi}^{\text{tar}}(x, t|s, a), t, s, a), \quad \psi_{\phi}^{\text{tar}}(x, 1|s, a) = x_1.$$

Solving this ODE from $t = 1$ to 2 yields the final target-domain prediction: $s' \doteq x_2 = \psi_{\phi}^{\text{tar}}(x_1, 2|s, a)$.

Theorem 3.1 (Conditions for Composite Flow Yielding Smaller Errors). *We assume the state space is bounded for both source and target domains, i.e., $|s| \leq \zeta \forall s \in \mathcal{S}$. For an unseen sample pair*

(s, a), there exists a constant $C > 0$ (independent of sample sizes and problem dimension) such that, the mean square error of the composite flow Err_{compst} is smaller than that of the direct flow Err_{direct} , i.e., $Err_{compst} < Err_{direct}$ whenever the total-variation distance obeys the explicit bound

$$D_{TV}(p_{src}(\cdot|s, a), p_{tar}(\cdot|s, a)) \leq \frac{C}{\zeta^2} \left(-\frac{\text{Tr}(\Sigma_{s'}^{src})}{\sqrt{N_{src}}} + \frac{\text{Tr}(\Sigma_{s'}^{tar})}{\sqrt{N_{tar}}} \right) \forall s, a,$$

where $\Sigma_{s'}^{tar}, \Sigma_{s'}^{src}$ are the covariance matrices of the N_{tar} samples collected in the target MDP and the N_{src} samples collected in the source MDP, respectively.

As shown in Theorem 3.1, if the distance between the source and target dynamics is below a certain threshold, our composite flow model achieves a smaller generalization error compared to directly learning the target flow from a Gaussian prior. This aligns with our setting: when the two dynamics deviates too large, leveraging source-domain data offers little benefit. Moreover, when the amount of target-domain data is limited (i.e., small N_{tar}), the tolerance for this distance becomes more relaxed—consistent with our setting where interaction with the target environment is scarce. The bound also becomes more relaxed with more source domain data (larger N_{src}), which aligns with our setting of having abundant source domain data.

To compute the Wasserstein distance between the source and target transition distributions, we can use the OT-FM objective to train the target flow, initialized from the source flow distribution. However, when the state-action pair (s, a) lies in a continuous space, it is not feasible to obtain a batch of samples corresponding to one (s, a) from the target domain.

To address this, we follow prior works [22, 17] that handle samples with distinct conditioning variables. The key idea is to incorporate the conditioning variables into the cost function when solving for the optimal transport coupling. Specifically, we define the cost between two sample pairs ($s_{src}, a_{src}, s'_{src}$) and ($s_{tar}, a_{tar}, s'_{tar}$) as:

$$c((s_{src}, a_{src}, s'_{src}, s_{tar}, a_{tar}, s'_{tar})) = \|s'_{src} - s'_{tar}\|_2^2 + \eta (\|s_{src} - s_{tar}\|_2^2 + \|a_{src} - a_{tar}\|_2^2),$$

where $\eta > 0$ is a weighting coefficient that controls the influence of the conditional terms.

Then the training objective of the target flow follows

$$\mathcal{L}_{tar}(\phi) = \mathbb{E}_{((s_{src}, a_{src}, s'_{src} \doteq x_1), (s_{tar}, a_{tar}, s'_{tar} \doteq x_2)) \sim q^*, t \sim \mathcal{U}[1, 2]} \left[\|v_\phi(x_t, t, s_t, a_t) - (s_{tar} - s_{src})\|_2^2 \right],$$

where q^* is the optimal coupling of empirical distribution ($s_{src}, a_{src}, s'_{src}$) generated by learned source flow and empirical transition ($s_{tar}, a_{tar}, s'_{tar}$) from target domain replay buffer. x_t is the linear interpolation between x_1 and x_2 , s_t is the interpolation between s_{src} and s_{tar} , and a_t is the interpolation between a_{src} and a_{tar} .

The complete training algorithms of the source flow and the target flow are in Appendix B.

Proposition 3.2 (Informal; shared-latent coupling is W_2 -optimal). Given (s, a) $\in \mathcal{S} \times \mathcal{A}$. As $\eta \rightarrow \infty$ and the training batch size $\rightarrow \infty$, the Wasserstein distance between the source and target transition distributions satisfies

$$W_2^2(p_{src}(\cdot|s, a), p_{tar}(\cdot|s, a)) = \mathbb{E}_{x_0 \sim \mathcal{N}(0, \mathbf{I})} \left[\|\psi_\theta^{src}(x_0, 1|s, a) - \psi_\phi^{tar}(\psi_\theta^{src}(x_0, 1|s, a), 2|s, a)\|_2^2 \right].$$

Monte Carlo Estimator. This result yields a practical Monte Carlo estimator of the *dynamics gap* $\Delta(s, a)$ using shared latent variables:

$$\widehat{\Delta}(s, a) = \left(\frac{1}{M} \sum_{j=1}^M \|\psi_\theta^{src}(x_0^{(j)}, 1|s, a) - \psi_\phi^{tar}(\psi_\theta^{src}(x_0^{(j)}, 1|s, a), 2|s, a)\|_2^2 \right)^{\frac{1}{2}}, \quad x_0^{(j)} \sim \mathcal{N}(0, \mathbf{I}). \quad (2)$$

3.2 Data Collection at High Dynamics Gap Region

As discussed in Section 2.1, using behavior cloning and augmenting the replay buffer with low dynamics gap source data can alleviate performance drop from distribution shift. However, relying solely on such data may limit state-action coverage and hinder policy learning. To address this, we propose a new data collection strategy.

At each training iteration, we construct the replay buffer by selectively incorporating source transitions with small estimated dynamics gap:

$$\mathcal{B} = \left\{ (s, a) \in \mathcal{D}_{\text{src}} : \widehat{\Delta}(s, a) \leq \tau \right\} \cup \mathcal{D}_{\text{tar}}, \quad (3)$$

where τ is a predefined threshold. To improve data diversity and encourage better generalization, we actively explore regions with high dynamics gap—areas likely underrepresented in the buffer due to the dominance of low-gap samples. We adopt an optimistic exploration policy that selects actions by

$$a = \arg \max_{a \in \mathcal{A}} \left[Q(s, a) + \beta \widehat{\Delta}(s, a) \right], \quad (4)$$

where β is a hyperparameter that trades off return and exploration of underexplored dynamics.

Theorem 3.3 (Large Dynamics Gap Exploration Reduces Performance Gap). *Compared to behavior cloning on the offline source dataset, training a policy $\hat{\pi}$ by replacing all source samples with a dynamics gap exceeding κ (as estimated by the composite flow) with target domain samples can reduce the performance gap to the optimal target policy π_{tar}^* by*

$$\Delta_{\kappa} = \frac{4L_r(1+\gamma)}{(1-\gamma)(1-\gamma L_p)} \left(\Delta_{W_2} - \kappa - \sqrt{\text{Var}(s'|\nu)_{\text{tar}} + O\left(\frac{\text{Tr}(\Sigma_{s'})}{\sqrt{N_{\text{tar}}}}\right)} \right) \quad (5)$$

Here L_r and L_p are the Lipschitz constants for the reward and transition function, respectively. $\gamma L_p < 1$. $\Delta_{W_2} := \sup_{s,a} W_2(p_{\text{src}}(\cdot|s, a), p_{\text{tar}}(\cdot|s, a))$ is the largest dynamics gap. $\text{Var}(s'|\nu)_{\text{tar}}$ is the conditional variance of s' given s, a under the distribution p_{tar} .

From Theorem 3.3, exploration in regions with high dynamics gap can reduce the performance gap relative to the optimal policy. The parameter κ serves as a threshold: the bound holds when the policy is trained without source samples whose dynamics gap exceeds κ . As β increases, more samples are collected from high-gap regions, which decreases κ . This increases the bound Δ_{κ} on performance gap reduction, resulting in a policy with higher expected return.

3.3 Practical Implementation

Our method can be instantiated using standard actor-critic algorithms with a critic $Q_{\zeta}(s, a)$ and a policy $\pi_{\varphi}(a|s)$. To incorporate the dynamics gap, we apply rejection sampling to retain a fixed percentage of source transitions with the lowest estimated gap in each iteration. The critic is trained by minimizing

$$\mathcal{L}_Q = \mathbb{E}_{(s,a,s') \sim \mathcal{D}_{\text{tar}}} [(Q_{\zeta}(s, a) - y)^2] + \mathbb{E}_{(s,a,s') \sim \mathcal{D}_{\text{src}}} [\mathbf{1}(\widehat{\Delta}(s, a) \leq \widehat{\Delta}_{\xi\%})(Q_{\zeta}(s, a) - y)^2], \quad (6)$$

where $\widehat{\Delta}_{\xi\%}$ is the ξ -quantile of the estimated dynamics gap in the source minibatch. The target value is $y = r + \gamma Q_{\zeta}(s', a') + \beta \widehat{\Delta}(s, a)$, with $a' \sim \pi_{\varphi}(\cdot|s')$.

The policy is updated using a combination of policy improvement and behavior cloning, with the following objective:

$$\mathcal{L}_{\pi} = \mathbb{E}_{s \sim \mathcal{D}_{\text{src}} \cup \mathcal{D}_{\text{tar}}, a \sim \pi_{\varphi}(\cdot|s)} [Q_{\zeta}(s, a)] - \omega \mathbb{E}_{(s,a) \sim \mathcal{D}_{\text{src}}, \tilde{a} \sim \pi_{\varphi}(\cdot|s)} [\|a - \tilde{a}\|^2], \quad (7)$$

where ω is a hyperparameter that balances policy improvement with imitation of source actions. The behavior cloning term encourages sampled actions from the policy to match those in the offline source dataset as suggested in Lemma 2.2.

The pseudocode of COMPFLOW, instantiated with Soft Actor-Critic (SAC) [18], is presented in Appendix C.

4 Related Work

Online RL with Offline Dataset. Online RL often requires extensive environment interactions [48, 62], which can be costly or impractical in real-world settings. To improve sample efficiency, Offline-to-Online RL leverages pre-collected offline data to bootstrap online learning [38]. A typical two-phase approach trains an initial policy offline, then fine-tunes it online [38, 28, 39]. However, conservative strategies used to mitigate distributional shift—such as pessimistic value estimation [27]—can produce suboptimal initial policies and hinder exploration [35, 39]. To resolve this

tension, recent methods propose ensemble-based pessimism [28], value calibration [39], optimistic action selection [28], and policy expansion [64]. Others directly incorporate offline data into the replay buffer of off-policy algorithms [3], improving stability via ensemble distillation and layer normalization. However, these works assume identical dynamics between the source and target environments. In contrast, our work explicitly addresses the dynamics shift between the offline and online environments.

Domain Adaptation for RL. Our setting aligns with domain adaptation, where the source and target domains share observation and action spaces but differ in transition dynamics. Prior work has addressed such discrepancies via system identification [8, 10, 5], domain randomization [50, 55, 36], imitation learning [23, 19], and meta-RL [37, 45], often assuming shared environment distributions [52] or requiring expert demonstrations. Recent methods emphasize dynamics-aware policy learning. One direction is *reward modification*, which penalizes source transitions unlikely under target dynamics by adjusting the reward function [12, 30] or down-weighting value estimates in high-gap regions [41]. Another is *data filtering*, which retains only source transitions with low estimated dynamics gap [59], using metrics such as transition probability ratios [12], mutual information [58], value inconsistency [59], or representation KL divergence [32]. However, these metrics can be ill-defined when dynamics have disjoint support, and value-based methods suffer from instability due to bootstrapping bias.

Our work differs from these approaches by leveraging the theoretical connection between optimal transport and flow matching, which enables principled estimation of the Wasserstein distance between source and target transition as the dynamics gap. A closely related work by [34] also employs optimal transport to quantify the dynamics gap. However, their setting assumes both the source and target domains are offline, and their estimation is based on the concatenated tuple (s, a, s') observed in the offline dataset, rather than computing a distance between the conditional transition distributions $p_{\text{src}}(s'|s, a)$ and $p_{\text{tar}}(s'|s, a)$. Consequently, their metric does not provide an accurate measure of the transition dynamics gap and cannot be directly used to compute exploration bonuses, which require dynamics gap estimation conditioned on a given state-action pair.

RL with Diffusion and Flow Models. Diffusion models [20, 51] and flow matching [29, 11] have emerged as powerful generative tools capable of modeling complex, high-dimensional distributions. Their application in RL is consequently expanding. Researchers have employed these generative models for various tasks, including planning and trajectory synthesis [21], representing expressive multimodal policies [7, 46], providing behavior regularization [6], or augmenting training datasets with synthesized experiences. While these works often focus on policy learning or modeling dynamics within a single environment, our approach targets the transfer learning setting. Specifically, we address scenarios characterized by a *dynamics gap* between source and target domains. We utilize Flow Matching, leveraging its connection to optimal transport, to estimate this gap.

5 Experiments

In this section, we evaluate our approach across a variety of environments featuring different types of dynamics shifts. We also perform ablation and hyperparameter studies to gain deeper insights into the design and behavior of COMPFLOW.

5.1 Experimental Setup

Tasks and datasets. We evaluate our algorithm under two types of dynamics shifts—morphology and kinematic—across three OpenAI Gym locomotion tasks: HalfCheetah, Hopper, and Walker2d [4]. Each experiment involves an offline source domain and an online target domain with modified transition dynamics following [33]. Morphology shifts change body part sizes, while kinematic shifts constrain joint angles. For each task, we use three D4RL source datasets—medium, medium-replay, and medium-expert—capturing varying data quality [16]. Additional results and environment details are in Appendix I and J.

Baselines. We compare COMPFLOW against the following baselines: BC-SAC extends SAC by incorporating both source and target data, with a behavior cloning (BC) term for the offline source. H2O [41] penalizes Q-values for state-action pairs with large dynamics gaps. BC-VGDF [59] selects source transitions with value targets consistent with the target domain and adds a BC term. BC-PAR [32] applies a reward penalty based on representation mismatch between source and target transitions, also including a BC term. Implementation details are provided in Appendix J.

Dataset	Task Name	BC-SAC	H2O	BC-VGDF	BC-PAR	Ours
MR	HalfCheetah (Morphology)	2495 ± 43	1430 ± 408	2765 ± 124	1790 ± 91	3119 ± 107
MR	HalfCheetah (Kinematic)	4868 ± 186	4257 ± 609	4392 ± 403	4179 ± 441	5189 ± 262
MR	Hopper (Morphology)	346 ± 4	361 ± 18	348 ± 21	354 ± 25	355 ± 6
MR	Hopper (Kinematic)	1024 ± 0	1025 ± 0	1024 ± 0	1024 ± 1	1024 ± 1
MR	Walker2D (Morphology)	598 ± 475	1014 ± 193	672 ± 576	458 ± 151	1094 ± 791
M	HalfCheetah (Morphology)	1522 ± 72	1720 ± 273	1829 ± 345	1427 ± 196	2282 ± 287
M	HalfCheetah (Kinematic)	5451 ± 195	5019 ± 773	4972 ± 381	5243 ± 120	5593 ± 44
M	Hopper (Morphology)	436 ± 45	410 ± 8	406 ± 52	418 ± 13	604 ± 173
M	Hopper (Kinematic)	1022 ± 1	970 ± 98	934 ± 43	1020 ± 3	1023 ± 2
M	Walker2D (Morphology)	457 ± 317	577 ± 201	584 ± 219	431 ± 177	886 ± 372
ME	HalfCheetah (Morphology)	1195 ± 241	1147 ± 169	1072 ± 102	1207 ± 53	1485 ± 67
ME	HalfCheetah (Kinematic)	4211 ± 262	5143 ± 330	4603 ± 498	4399 ± 164	5750 ± 84
ME	Hopper (Morphology)	349 ± 47	444 ± 15	357 ± 63	407 ± 28	462 ± 89
ME	Hopper (Kinematic)	1024 ± 1	1031 ± 3	1022 ± 3	1027 ± 8	1022 ± 2
ME	Walker2D (Morphology)	429 ± 117	1103 ± 444	502 ± 301	380 ± 231	648 ± 180
Average Return		1695	1710	1699	1584	2036

Table 1: Comparison of performance under different dynamics shift scenarios and dataset types after 40K environment interactions. MR=Medium Replay, M = Medium, ME = Medium Expert. We mark a cell green if the method achieves the highest average return and improves over the second-best by at least 2%. Yellow highlights indicate practical ties (within 2% of the top method).

5.2 Main Results

We evaluate the return of each algorithm in the target domain after 40K environment interactions and 400K gradient steps, reflecting the limited interaction setting. The performance of all methods is reported in Table 1. Our key findings are summarized as follows:

(1) COMPFLOW consistently outperforms recent off-dynamics RL baselines across varying dataset qualities and types of dynamics shifts. Specifically, it achieves the highest return on **10 out of 15** tasks and ties on **4**. On average, COMPFLOW attains a score of **2036**, while the second-best baseline, H2O, achieves only **1710**.

(2) COMPFLOW significantly outperforms the base algorithm BC-SAC in most scenarios. Notably, COMPFLOW achieves higher returns than BC-SAC on **12 out of 15** tasks under both morphology and kinematic shifts, and achieves ties on the remaining 3 tasks. On average, COMPFLOW yields an improvement of **20.1%** over BC-SAC, clearly validating the effectiveness of our method.

(3) Additionally, we observe that recent baselines often perform similarly to BC-SAC across many tasks, consistent with the findings in [33], suggesting that they fail to effectively leverage the offline source domain data. This may stem from methods like H2O and BC-PAR relying on KL divergence or mutual information, which can be ill-defined under large dynamics gaps or disjoint supports. Meanwhile, BC-VGDF adopts a data filtering strategy based on estimated value functions, which is often more challenging than learning transition dynamics due to bootstrapping bias and target non-stationarity. In contrast, our method, COMPFLOW, leverages flow matching to model complex transition dynamics and exploits its theoretical connection to optimal transport to estimate the dynamics gap via Wasserstein distance—a more robust and principled metric.

5.3 Ablation and Hyperparameter Analysis

Composite Flow. We first evaluate the effectiveness of the proposed composite flow matching design. For comparison, we train a direct flow model on the target domain initialized from a Gaussian prior. We compute the mean squared error (MSE) on a held-out 10% validation set and report the average MSE across different epochs during RL training. As shown in Figure 3, the composite flow significantly reduces the MSE of the transition dynamics on the target

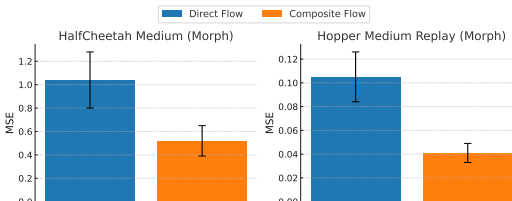


Figure 3: Comparison of MSE between direct flow and composite flow.

domain. This improvement stems from its ability to reuse structural knowledge learned from the source domain, where abundant data is available. These empirical findings support the theoretical insight presented in Theorem 3.1 that our composite flow can improve the generalization ability.

Impact of data selection ratio $\xi\%$. The data selection ratio ξ decides how many source domain data in a sampled batch can be shared for policy training. A larger ξ indicates that more source domain data will be admitted. To examine its influence, We sweep ξ across $\{70, 50, 30, 20\}$. The results is shown in Figure 4. Although the optimal ξ seems task dependent, moderate values of ξ (e.g., 30 or 50) generally yield good performance across tasks, striking a balance between leveraging useful source data and avoiding high dynamics mismatch. When ξ is too large (e.g., 70), performance often degrades—particularly in Walker Medium (Morph) and Walker Medium Replay (Morph)—likely due to the inclusion of low-quality transitions with large dynamics gap. HalfCheetah consistently achieves higher returns compared to other domains, suggesting that knowledge transfer and policy learning in this environment are easier. Consequently, overly conservative filtering (e.g., $\xi = 20$) may exclude valuable source data, leading to slower learning. In this case, allowing more source data (e.g., $\xi = 70$) appears beneficial.

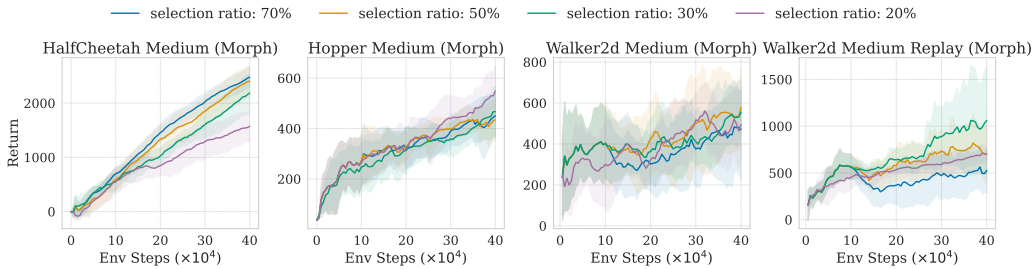


Figure 4: Comparison of return under different data selection ratios across tasks.

Impact of exploration strength β . β controls the strength of exploration toward regions with large dynamics gap. A large β indicates higher incentive to explore such regions. As shown in Figure 5, the effect of β on return is task-dependent, possibly due to differences in the underlying MDPs. In the Friction tasks, we observe that larger exploration bonuses lead to higher asymptotic returns. This suggests that incentivizing exploration helps the algorithm discover high-reward regions more effectively. In contrast, in the Morphology tasks, moderate values of β typically outperform both smaller and larger values. This indicates that excessive exploration may not be effective in some tasks. While the optimal β varies by task, one trend is consistent: across all five experiments, the setting with no exploration ($\beta = 0$) consistently ranks as the lowest or the second lowest performers. This empirical finding confirms the importance of the exploration bonus and provides evidence supporting our algorithmic design.

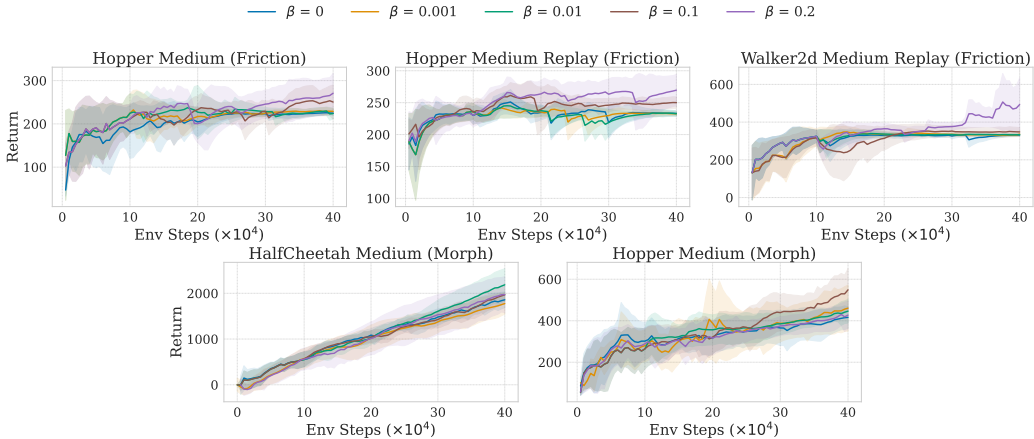


Figure 5: Comparison of return under different exploration strengths across tasks.

6 Conclusion and Limitations

In this paper, we proposed COMPFLOW, a new method for estimating the dynamics gap in reinforcement learning with shifted-dynamics data. COMPFLOW leverages the theoretical connection between flow matching and optimal transport. To address data scarcity in the target domain, we adopt a composite flow structure that builds the target flow model on top of the output distribution from the source domain flow. This composite formulation improves generalization and enables the use of Wasserstein distance between source and target transitions as a robust measure of the dynamics gap. Using this principled estimation, we further encourage the policy to explore regions with high dynamics gap and provide a theoretical analysis of the benefits. Empirically, we demonstrate that COMPFLOW consistently outperforms or matches state-of-the-art baselines across 15 diverse RL tasks with varying types of dynamics shift.

Limitations. (1) COMPFLOW is currently limited to settings where the source and target domains share the same state and action spaces. (2) Our evaluation is confined to simulated environments; evaluating COMPFLOW in real-world scenarios remains an important direction for future work. (3) Extending COMPFLOW to multi-domain transfer settings is also a promising avenue for exploration.

References

- [1] Michael Samuel Albergo and Eric Vanden-Eijnden. Building normalizing flows with stochastic interpolants. In *The Eleventh International Conference on Learning Representations*, 2023. URL <https://openreview.net/forum?id=li7qeBbCR1t>.
- [2] Martin Arjovsky, Soumith Chintala, and Léon Bottou. Wasserstein gan. In *International Conference on Machine Learning*, pages 214–223. PMLR, 2017.
- [3] Philip J Ball, Laura Smith, Ilya Kostrikov, and Sergey Levine. Efficient online reinforcement learning with offline data. In *International Conference on Machine Learning*, pages 1577–1594. PMLR, 2023.
- [4] Greg Brockman, Vicki Cheung, Ludwig Pettersson, Jonas Schneider, John Schulman, Jie Tang, and Wojciech Zaremba. Openai gym. *arXiv preprint arXiv:1606.01540*, 2016.
- [5] Yevgen Chebotar, Ankur Handa, Viktor Makoviychuk, Miles Macklin, Jan Issac, Nathan Ratliff, and Dieter Fox. Closing the sim-to-real loop: Adapting simulation randomization with real world experience. In *2019 International Conference on Robotics and Automation (ICRA)*, pages 8973–8979. IEEE, 2019.
- [6] Huayu Chen, Cheng Lu, Zhengyi Wang, Hang Su, and Jun Zhu. Score regularized policy optimization through diffusion behavior. In *The Twelfth International Conference on Learning Representations*, 2024. URL <https://openreview.net/forum?id=xCRr9Dro1J>.
- [7] Cheng Chi, Siyuan Feng, Yilun Du, Zhenjia Xu, Eric Cousineau, Benjamin Burchfiel, and Shuran Song. Diffusion policy: Visuomotor policy learning via action diffusion. In *Proceedings of Robotics: Science and Systems (RSS)*, 2023.
- [8] Ignasi Clavera, Anusha Nagabandi, Ronald S Fearing, Pieter Abbeel, Sergey Levine, and Chelsea Finn. Learning to adapt: Meta-learning for model-based control. *arXiv preprint arXiv:1803.11347*, 3:3, 2018.
- [9] Marco Cuturi. Sinkhorn distances: Lightspeed computation of optimal transport. *Advances in neural information processing systems*, 26, 2013.
- [10] Yuqing Du, Olivia Watkins, Trevor Darrell, Pieter Abbeel, and Deepak Pathak. Auto-tuned sim-to-real transfer. In *2021 IEEE International Conference on Robotics and Automation (ICRA)*, pages 1290–1296. IEEE, 2021.
- [11] Patrick Esser, Sumith Kulal, Andreas Blattmann, Rahim Entezari, Jonas Müller, Harry Saini, Yam Levi, Dominik Lorenz, Axel Sauer, Frederic Boesel, et al. Scaling rectified flow transformers for high-resolution image synthesis. In *Forty-first international conference on machine learning*, 2024.
- [12] Benjamin Eysenbach, Swapnil Asawa, Shreyas Chaudhari, Sergey Levine, and Ruslan Salakhutdinov. Off-dynamics reinforcement learning: Training for transfer with domain classifiers. *arXiv preprint arXiv:2006.13916*, 2020.

- [13] Kilian Fatras, Younes Zine, Rémi Flamary, Rémi Gribonval, and Nicolas Courty. Learning with minibatch wasserstein: asymptotic and gradient properties. *arXiv preprint arXiv:1910.04091*, 2019.
- [14] Kilian Fatras, Younes Zine, Szymon Majewski, Rémi Flamary, Rémi Gribonval, and Nicolas Courty. Minibatch optimal transport distances; analysis and applications. *arXiv preprint arXiv:2101.01792*, 2021.
- [15] Rémi Flamary, Nicolas Courty, Alexandre Gramfort, Mokhtar Z. Alaya, Aurélie Boisbunon, Stanislas Chambon, Laetitia Chapel, Adrien Corenflos, Kilian Fatras, Nemo Fournier, Léo Gautheron, Nathalie T.H. Gayraud, Hicham Janati, Alain Rakotomamonjy, Ievgen Redko, Antoine Rolet, Antony Schutz, Vivien Seguy, Danica J. Sutherland, Romain Tavenard, Alexander Tong, and Titouan Vayer. Pot: Python optimal transport. *Journal of Machine Learning Research*, 22(78):1–8, 2021. URL <http://jmlr.org/papers/v22/20-451.html>.
- [16] Justin Fu, Aviral Kumar, Ofir Nachum, George Tucker, and Sergey Levine. D4rl: Datasets for deep data-driven reinforcement learning, 2020.
- [17] Adam P Generale, Andreas E Robertson, and Surya R Kalidindi. Conditional variable flow matching: Transforming conditional densities with amortized conditional optimal transport. *arXiv preprint arXiv:2411.08314*, 2024.
- [18] Tuomas Haarnoja, Aurick Zhou, Pieter Abbeel, and Sergey Levine. Soft actor-critic: Off-policy maximum entropy deep reinforcement learning with a stochastic actor. In *International conference on machine learning*, pages 1861–1870. Pmlr, 2018.
- [19] Donald Hejna, Lerrel Pinto, and Pieter Abbeel. Hierarchically decoupled imitation for morphological transfer. In *International Conference on Machine Learning*, pages 4159–4171. PMLR, 2020.
- [20] Jonathan Ho, Ajay Jain, and Pieter Abbeel. Denoising diffusion probabilistic models. *Advances in neural information processing systems*, 33:6840–6851, 2020.
- [21] Michael Janner, Yilun Du, Joshua Tenenbaum, and Sergey Levine. Planning with diffusion for flexible behavior synthesis. In *International Conference on Machine Learning*, pages 9902–9915. PMLR, 2022.
- [22] Gavin Kerrigan, Giosue Migliorini, and Padhraic Smyth. Dynamic conditional optimal transport through simulation-free flows. In *The Thirty-eighth Annual Conference on Neural Information Processing Systems*, 2024. URL <https://openreview.net/forum?id=tk0uaRynhH>.
- [23] Kuno Kim, Yihong Gu, Jiaming Song, Shengjia Zhao, and Stefano Ermon. Domain adaptive imitation learning. In *International Conference on Machine Learning*, pages 5286–5295. PMLR, 2020.
- [24] Diederik P Kingma and Jimmy Ba. Adam: A method for stochastic optimization. *International Conference on Representation Learning*, 2015.
- [25] Jens Kober, J Andrew Bagnell, and Jan Peters. Reinforcement learning in robotics: A survey. *The International Journal of Robotics Research*, 32(11):1238–1274, 2013.
- [26] Ling kai Kong, Haichuan Wang, Yuqi Pan, Cheol Woo Kim, Mingxiao Song, Alayna Nguyen, Tonghan Wang, Haifeng Xu, and Milind Tambe. Robust optimization with diffusion models for green security. *arXiv preprint arXiv:2503.05730*, 2025.
- [27] Aviral Kumar, Aurick Zhou, George Tucker, and Sergey Levine. Conservative q-learning for offline reinforcement learning. *Advances in neural information processing systems*, 33: 1179–1191, 2020.
- [28] Seunghyun Lee, Younggyo Seo, Kimin Lee, Pieter Abbeel, and Jinwoo Shin. Offline-to-online reinforcement learning via balanced replay and pessimistic q-ensemble. In *Conference on Robot Learning*, pages 1702–1712. PMLR, 2022.
- [29] Yaron Lipman, Ricky T. Q. Chen, Heli Ben-Hamu, Maximilian Nickel, and Matthew Le. Flow matching for generative modeling. In *The Eleventh International Conference on Learning Representations*, 2023. URL <https://openreview.net/forum?id=PqvMRDCJT9t>.
- [30] Jinxin Liu, Hongyin Zhang, and Donglin Wang. Dara: Dynamics-aware reward augmentation in offline reinforcement learning. *arXiv preprint arXiv:2203.06662*, 2022.

- [31] Xingchao Liu, Chengyue Gong, and Qiang Liu. Flow straight and fast: Learning to generate and transfer data with rectified flow. *arXiv preprint arXiv:2209.03003*, 2022.
- [32] Jiafei Lyu, Chenjia Bai, Jingwen Yang, Zongqing Lu, and Xiu Li. Cross-domain policy adaptation by capturing representation mismatch. *arXiv preprint arXiv:2405.15369*, 2024.
- [33] Jiafei Lyu, Kang Xu, Jiacheng Xu, Jing-Wen Yang, Zongzhang Zhang, Chenjia Bai, Zongqing Lu, Xiu Li, et al. Odr1: A benchmark for off-dynamics reinforcement learning. *Advances in Neural Information Processing Systems*, 37:59859–59911, 2024.
- [34] Jiafei Lyu, Mengbei Yan, Zhongjian Qiao, Runze Liu, Xiaoteng Ma, Deheng Ye, Jing-Wen Yang, Zongqing Lu, and Xiu Li. Cross-domain offline policy adaptation with optimal transport and dataset constraint. In *The Thirteenth International Conference on Learning Representations*, 2025.
- [35] Max Sobol Mark, Ali Ghadirzadeh, Xi Chen, and Chelsea Finn. Fine-tuning offline policies with optimistic action selection. In *Deep Reinforcement Learning Workshop NeurIPS 2022*, 2022.
- [36] Bhairav Mehta, Manfred Diaz, Florian Golemo, Christopher J Pal, and Liam Paull. Active domain randomization. In *Conference on Robot Learning*, pages 1162–1176. PMLR, 2020.
- [37] Anusha Nagabandi, Ignasi Clavera, Simin Liu, Ronald S Fearing, Pieter Abbeel, Sergey Levine, and Chelsea Finn. Learning to adapt in dynamic, real-world environments through meta-reinforcement learning. *arXiv preprint arXiv:1803.11347*, 2018.
- [38] Ashvin Nair, Abhishek Gupta, Murtaza Dalal, and Sergey Levine. Awac: Accelerating online reinforcement learning with offline datasets. *arXiv preprint arXiv:2006.09359*, 2020.
- [39] Mitsuhiro Nakamoto, Simon Zhai, Anikait Singh, Max Sobol Mark, Yi Ma, Chelsea Finn, Aviral Kumar, and Sergey Levine. Cal-ql: Calibrated offline rl pre-training for efficient online fine-tuning. *Advances in Neural Information Processing Systems*, 36:62244–62269, 2023.
- [40] Ariel Neufeld and Julian Sester. Bounding the difference between the values of robust and non-robust markov decision problems. *Journal of Applied Probability*, pages 1–14, 2023.
- [41] Haoyi Niu, Yiwen Qiu, Ming Li, Guyue Zhou, Jianming Hu, Xianyuan Zhan, et al. When to trust your simulator: Dynamics-aware hybrid offline-and-online reinforcement learning. *Advances in Neural Information Processing Systems*, 35:36599–36612, 2022.
- [42] Aram-Alexandre Pooladian, Heli Ben-Hamu, Carles Domingo-Enrich, Brandon Amos, Yaron Lipman, and Ricky TQ Chen. Multisample flow matching: Straightening flows with minibatch couplings. *arXiv preprint arXiv:2304.14772*, 2023.
- [43] Ben Poole, Sherjil Ozair, Aaron Van Den Oord, Alex Alemi, and George Tucker. On variational bounds of mutual information. In *International Conference on Machine Learning*, pages 5171–5180. PMLR, 2019.
- [44] Chengrui Qu, Laixi Shi, Kishan Panaganti, Pengcheng You, and Adam Wierman. Hybrid transfer reinforcement learning: Provable sample efficiency from shifted-dynamics data. In *The 28th International Conference on Artificial Intelligence and Statistics*, 2025. URL <https://openreview.net/forum?id=ndWOLqVRHC>.
- [45] Roberta Raileanu, Max Goldstein, Arthur Szlam, and Rob Fergus. Fast adaptation to new environments via policy-dynamics value functions. In *Proceedings of the 37th International Conference on Machine Learning*, pages 7920–7931, 2020.
- [46] Allen Z. Ren, Justin Lidard, Lars Lien Ankile, Anthony Simeonov, Pulkit Agrawal, Anirudha Majumdar, Benjamin Burchfiel, Hongkai Dai, and Max Simchowitz. Diffusion policy optimization. In *The Thirteenth International Conference on Learning Representations*, 2025. URL <https://openreview.net/forum?id=mEpqHvbD2h>.
- [47] Julian Schrittwieser, Ioannis Antonoglou, Thomas Hubert, Karen Simonyan, Laurent Sifre, Simon Schmitt, Arthur Guez, Edward Lockhart, Demis Hassabis, Thore Graepel, et al. Mastering atari, go, chess and shogi by planning with a learned model. *Nature*, 588(7839):604–609, 2020.
- [48] David Silver, Aja Huang, Chris J Maddison, Arthur Guez, Laurent Sifre, George Van Den Driessche, Julian Schrittwieser, Ioannis Antonoglou, Veda Panneershelvam, Marc Lanctot, et al. Mastering the game of go with deep neural networks and tree search. *nature*, 529(7587):484–489, 2016.

- [49] David Silver, Julian Schrittwieser, Karen Simonyan, Ioannis Antonoglou, Aja Huang, Arthur Guez, Thomas Hubert, Lucas Baker, Matthew Lai, Adrian Bolton, et al. Mastering the game of go without human knowledge. *nature*, 550(7676):354–359, 2017.
- [50] Reda Bahi Slaoui, William R Clements, Jakob N Foerster, and Sébastien Toth. Robust domain randomization for reinforcement learning. 2019.
- [51] Yang Song, Jascha Sohl-Dickstein, Diederik P Kingma, Abhishek Kumar, Stefano Ermon, and Ben Poole. Score-based generative modeling through stochastic differential equations. *arXiv preprint arXiv:2011.13456*, 2020.
- [52] Yuda Song, Aditi Mavalankar, Wen Sun, and Sicun Gao. Provably efficient model-based policy adaptation. *arXiv preprint arXiv:2006.08051*, 2020.
- [53] Yuda Song, Yifei Zhou, Ayush Sekhari, J Andrew Bagnell, Akshay Krishnamurthy, and Wen Sun. Hybrid rl: Using both offline and online data can make rl efficient. *arXiv preprint arXiv:2210.06718*, 2022.
- [54] Chen Tang, Ben Abbatematteo, Jiaheng Hu, Rohan Chandra, Roberto Martín-Martín, and Peter Stone. Deep reinforcement learning for robotics: A survey of real-world successes. In *Proceedings of the AAAI Conference on Artificial Intelligence*, volume 39, pages 28694–28698, 2025.
- [55] Josh Tobin, Rachel Fong, Alex Ray, Jonas Schneider, Wojciech Zaremba, and Pieter Abbeel. Domain randomization for transferring deep neural networks from simulation to the real world. In *2017 IEEE/RSJ international conference on intelligent robots and systems (IROS)*, pages 23–30. IEEE, 2017.
- [56] Emanuel Todorov, Tom Erez, and Yuval Tassa. Mujoco: A physics engine for model-based control. In *2012 IEEE/RSJ international conference on intelligent robots and systems*, pages 5026–5033. IEEE, 2012.
- [57] Tonghan Wang, Heng Dong, Yanchen Jiang, David C Parkes, and Milind Tambe. On diffusion models for multi-agent partial observability: Shared attractors, error bounds, and composite flow. *arXiv preprint arXiv:2410.13953*, 2024.
- [58] Xiaoyu Wen, Chenjia Bai, Kang Xu, Xudong Yu, Yang Zhang, Xuelong Li, and Zhen Wang. Contrastive representation for data filtering in cross-domain offline reinforcement learning. *arXiv preprint arXiv:2405.06192*, 2024.
- [59] Kang Xu, Chenjia Bai, Xiaoteng Ma, Dong Wang, Bin Zhao, Zhen Wang, Xuelong Li, and Wei Li. Cross-domain policy adaptation via value-guided data filtering. *Advances in Neural Information Processing Systems*, 36:73395–73421, 2023.
- [60] Lily Xu, Elizabeth Bondi, Fei Fang, Andrew Perrault, Kai Wang, and Milind Tambe. Dual-mandate patrols: Multi-armed bandits for green security. In *Proceedings of the AAAI Conference on Artificial Intelligence*, volume 35, pages 14974–14982, 2021.
- [61] Lily Xu, Andrew Perrault, Fei Fang, Haipeng Chen, and Milind Tambe. Robust reinforcement learning under minimax regret for green security. In *Uncertainty in Artificial Intelligence*, pages 257–267. PMLR, 2021.
- [62] Deheng Ye, Guibin Chen, Wen Zhang, Sheng Chen, Bo Yuan, Bo Liu, Jia Chen, Zhao Liu, Fuhao Qiu, Hongsheng Yu, et al. Towards playing full moba games with deep reinforcement learning. *Advances in Neural Information Processing Systems*, 33:621–632, 2020.
- [63] Chao Yu, Jiming Liu, Shamim Nemati, and Guosheng Yin. Reinforcement learning in healthcare: A survey. *ACM Computing Surveys (CSUR)*, 55(1):1–36, 2021.
- [64] Haichao Zhang, We Xu, and Haonan Yu. Policy expansion for bridging offline-to-online reinforcement learning. *arXiv preprint arXiv:2302.00935*, 2023.

Appendix for Composite Flow Matching for Reinforcement Learning with Shifted-Dynamics Data

A	Broader Impacts	14
B	Algorithms of Training Optimal Transport Flow Matching	14
C	Algorithms of Training Source and Target Flows	15
D	Algorithm of COMPFLOW built on Soft-Actor-Critic	16
E	Proof of Lemma 2.2	18
F	Proof of Theorem 3.1	19
G	Proof of Theorem 3.3	21
H	Proof of Proposition 3.2	23
I	Additional Experimental Results	24
	I.1 Additional Main Results	24
J	Experimental Details	24
	J.1 Environment Setting	25
	J.2 Implementation Details	26

A Broader Impacts

Our work aims to make reinforcement learning more practical in real-world domains—such as healthcare, robotics, and conservation—where online interaction is costly or unsafe. By addressing dynamics shifts between offline and online environments, our method enables more reliable and sample-efficient policy learning. This can support safer deployment in high-stakes settings, such as clinical decision support or adaptive anti-poaching strategies. However, we emphasize that policies trained on historical data should be used with caution, as misaligned dynamics or biased datasets may lead to unintended outcomes if not properly validated.

B Algorithms of Training Optimal Transport Flow Matching

The full training algorithm of Optimal Transport Flow Matching is given in Algorithm 1.

Algorithm 1 Training Optimal Transport Flow Matching

Require: Dataset D , batch size k , cost function $c(\cdot, \cdot)$, learning rate lr , flow model v_θ

1: **while** not converged **do**

2: Sample latent batch $\{x_0^{(i)}\}_{i=1}^k \sim \mathcal{N}(0, \mathbf{I})$

3: Sample data batch $\{x_1^{(j)}\}_{j=1}^k \sim D$

4: Compute optimal transport plan:

$$A \doteq \arg \min_{A \in B_k} \sum_{i,j} A(i,j) \cdot c(x_0^{(i)}, x_1^{(j)}), \quad c(x_0^{(i)}, x_1^{(j)}) = \|x_0^{(i)} - x_1^{(j)}\|_2^2$$

$\triangleright B_k$: set of $k \times k$ doubly-stochastic matrices

5: Sample k index pairs $\{(i_\ell, j_\ell)\}_{\ell=1}^k \sim A(i, j)$

6: Sample interpolation times $\{t^{(\ell)}\}_{\ell=1}^k \sim \mathcal{U}[0, 1]$

7: **for** $\ell = 1$ to k **do**

8: Define matched pair:

$$x_0^{(\ell)} \doteq x_0^{(i_\ell)}, \quad x_1^{(\ell)} \doteq x_1^{(j_\ell)}$$

9: Interpolate:

$$x_t^{(\ell)} \doteq t^{(\ell)} x_1^{(\ell)} + (1 - t^{(\ell)}) x_0^{(\ell)}$$

10: Compute target velocity:

$$v^{*(\ell)} \doteq x_1^{(\ell)} - x_0^{(\ell)}$$

11: **end for**

12: Compute loss:

$$\mathcal{L} \doteq \frac{1}{k} \sum_{\ell=1}^k \left\| v_\theta(x_t^{(\ell)}, t^{(\ell)}) - v^{*(\ell)} \right\|_2^2$$

13: Update parameters:

$$\theta \leftarrow \theta - \text{lr} \nabla_\theta \mathcal{L}$$

14: **end while**

15: **return** θ

C Algorithms of Training Source and Target Flows

The full training algorithms of the source flow and target flow are given in Algorithm 2 and Algorithm 3 respectively.

Algorithm 2 Training of Source Domain Flow Matching

Require: Source domain dataset D_{src} , batch size k , flow model v_θ , learning rate lr

1: **while** not converged **do**

2: Sample a batch of transitions $\{(s^{(i)}, a^{(i)}, s'^{(i)})\}_{i=1}^k \sim D_{\text{src}}$

3: For each i , define target sample $x_1^{(i)} \doteq (s^{(i)}, a^{(i)}, s'^{(i)})$

4: Sample $\{x_0^{(i)}\}_{i=1}^k \sim \mathcal{N}(0, \mathbf{I})$

5: Sample interpolation times $\{t^{(i)}\}_{i=1}^k \sim \mathcal{U}[0, 1]$

6: **for** $i = 1$ to k **do**

7: Compute interpolated point: $x_t^{(i)} = t^{(i)} x_1^{(i)} + (1 - t^{(i)}) x_0^{(i)}$

8: Compute target velocity: $v_i^* = x_1^{(i)} - x_0^{(i)}$

9: **end for**

10: Compute training loss:

$$\mathcal{L} = \frac{1}{k} \sum_{i=1}^k \left\| v_\theta(x_t^{(i)}, t^{(i)}, s^{(i)}, a^{(i)}) - v_i^* \right\|_2^2$$

11: Update $\theta \leftarrow \theta - \text{lr} \nabla_\theta \mathcal{L}$

12: **end while**

13: **return** Trained parameters θ

Algorithm 3 Training of Target Domain Flow via Optimal Transport

Require: Pre-trained source flow model $\psi_\theta(x, t \mid s, a)$, source dataset D_{src} , target dataset D_{tar} , batch size k , cost function $c(\cdot)$, regularization weight η , learning rate lr , target flow model v_ϕ

1: **while** not converged **do**

2: Sample latent vectors $\{x_0^{(i)}\}_{i=1}^k \sim \mathcal{N}(0, \mathbf{I})$

3: Sample source batch $\{s_{\text{src}}^{(i)}, a_{\text{src}}^{(i)}\}_{i=1}^k \sim D_{\text{src}}$

4: **for** $i = 1$ to k **do**

5: Predict source next state:

$$s_{\text{src}}^{\prime(i)} \doteq x_1^{(i)} \doteq \psi_\theta(x_0^{(i)}, 1 \mid s_{\text{src}}^{(i)}, a_{\text{src}}^{(i)})$$

6: **end for**

7: Sample target batch $\{s_{\text{tar}}^{(j)}, a_{\text{tar}}^{(j)}, s_{\text{tar}}^{\prime(j)}\}_{j=1}^k \sim D_{\text{tar}}$

8: Define $x_2^{(j)} \doteq s_{\text{tar}}^{\prime(j)}$

9: Compute optimal transport plan:

$$A \doteq \arg \min_{A \in B_k} \sum_{i,j} A(i, j) \cdot c(i, j)$$

10: where the cost is:

$$c(i, j) \doteq \|x_1^{(i)} - x_2^{(j)}\|_2^2 + \eta \left(\|s_{\text{src}}^{(i)} - s_{\text{tar}}^{(j)}\|_2^2 + \|a_{\text{src}}^{(i)} - a_{\text{tar}}^{(j)}\|_2^2 \right)$$

▷ B_k : set of $k \times k$ doubly-stochastic matrices

11: Sample k index pairs $\{(i_\ell, j_\ell)\}_{\ell=1}^k \sim A(i, j)$

12: Sample interpolation times $\{t^{(\ell)}\}_{\ell=1}^k \sim \mathcal{U}[1, 2]$ ▷ Time t for the target flow is from 1 to 2

13: **for** $\ell = 1$ to k **do**

14: Compute:

$$\begin{aligned} x_t^{(\ell)} &\doteq (t^{(\ell)} - 1)x_2^{(i_\ell)} + (2 - t^{(\ell)})x_1^{(j_\ell)} \\ s_t^{(\ell)} &\doteq (t^{(\ell)} - 1)s_{\text{tar}}^{(i_\ell)} + (2 - t^{(\ell)})s_{\text{src}}^{(j_\ell)} \\ a_t^{(\ell)} &\doteq (t^{(\ell)} - 1)a_{\text{tar}}^{(i_\ell)} + (2 - t^{(\ell)})a_{\text{src}}^{(j_\ell)} \\ v^{*(\ell)} &\doteq x_2^{(j_\ell)} - x_1^{(i_\ell)} \end{aligned}$$

15: **end for**

16: Compute training loss:

$$\mathcal{L} \doteq \frac{1}{k} \sum_{\ell=1}^k \left\| v_\phi(x_t^{(\ell)}, t^{(\ell)}, s_t^{(\ell)}, a_t^{(\ell)}) - v^{*(\ell)} \right\|_2^2$$

17: Update parameters:

$$\phi \leftarrow \phi - \text{lr} \nabla_\phi \mathcal{L}$$

18: **end while**

19: **return** ϕ

D Algorithm of COMPFLOW built on Soft-Actor-Critic

The full training algorithm of COMPFLOW built on SAC is given in Algorithm 4.

Algorithm 4 COMPFLOW built on Soft Actor-Critic (SAC)

- 1: **Input:** Source dataset D_{src} , target environment \mathcal{M}_{tar} , max interaction steps T_{max} , target model training frequency train_freq , source data selection ratio ξ , gap reward scale β , batch size B , behavior cloning weight ω , warmup steps warmup_steps , learning rate lr , target update rate ϖ
 - 2: **Initialization:** Policy π_φ , Q-functions $\{Q_{\zeta_i}\}_{i=1,2}$, target Q-functions $\{Q_{\zeta_i}^{\text{tgt}}\}_{i=1,2} \leftarrow \{Q_{\zeta_i}\}_{i=1,2}$, target replay buffer D_{tar}
 - 3: Pretrain source flow model $\psi_\theta(x, t \mid s, a)$ on D_{src} via Algorithm 2
 - 4: **for** $t = 1$ to T_{max} **do**
 - 5: Sample transition $(s_{\text{tar}}, a_{\text{tar}}, r_{\text{tar}}, s'_{\text{tar}}) \sim \mathcal{M}_{\text{tar}}$ using policy π_φ
 - 6: Update replay buffer: $D_{\text{tar}} \leftarrow D_{\text{tar}} \cup \{(s_{\text{tar}}, a_{\text{tar}}, r_{\text{tar}}, s'_{\text{tar}})\}$
 - 7: **if** $t \bmod \text{train_freq} = 0$ and $t > \text{warmup_steps}$ **then**
 - 8: Train target flow $\psi_\varphi(x, t \mid s, a)$ on D_{tar} via Algorithm 3
 - 9: **end if**
 - 10: **for** $k = 1$ to K **do**
 - 11: Sample $b_{\text{src}} = \{(s_{\text{src}}^{(i)}, a_{\text{src}}^{(i)}, r_{\text{src}}^{(i)}, s'_{\text{src}}{}^{(i)})\}_{i=1}^B \sim D_{\text{src}}$
 - 12: Sample $b_{\text{tar}} = \{(s_{\text{tar}}^{(i)}, a_{\text{tar}}^{(i)}, r_{\text{tar}}^{(i)}, s'_{\text{tar}}{}^{(i)})\}_{i=1}^B \sim D_{\text{tar}}$
 - 13: Estimate $\hat{\Delta}(s_{\text{src}}^{(i)}, a_{\text{src}}^{(i)})$ for each $(s_{\text{src}}^{(i)}, a_{\text{src}}^{(i)}) \in b_{\text{src}}$ via Eq. 2
 - 14: Select top $\xi\%$ of b_{src} with lowest gap: \tilde{b}_{src}
 - 15: For each $(s, a, r) \in \tilde{b}_{\text{src}}$, update reward: $r \leftarrow r + \beta \hat{\Delta}(s, a)$
 - 16: **for** $i = 1, 2$ **do**
 - 17: Compute Bellman target using target Q-networks:
$$y = r + \gamma \mathbb{E}_{a' \sim \pi_\varphi(\cdot | s')} \left[\min_{j=1,2} Q_{\zeta_j}^{\text{tgt}}(s', a') - \alpha \log \pi_\varphi(a' | s') \right]$$
 - 18: Compute Q-function loss gradient:
$$\begin{aligned} \nabla_{\zeta_i} \mathcal{L}_Q \leftarrow & \frac{1}{B} \sum_{(s^{\text{tar}}, a^{\text{tar}}, s'^{\text{tar}}, r^{\text{tar}}) \in b_{\text{tar}}} \nabla_{\zeta_i} (Q_{\zeta_i}(s^{\text{tar}}, a^{\text{tar}}) - y)^2 \\ & + \frac{1}{|\tilde{b}_{\text{src}}|} \sum_{(s^{\text{src}}, a^{\text{src}}, s'^{\text{src}}, r^{\text{src}}) \in \tilde{b}_{\text{src}}} \nabla_{\zeta_i} (Q_{\zeta_i}(s^{\text{src}}, a^{\text{src}}) - y)^2 \end{aligned}$$
 - 19: Update Q-network: $\zeta_i \leftarrow \zeta_i - \text{lr} \nabla_{\zeta_i} \mathcal{L}_Q$
 - 20: **end for**
 - 21: # Soft update of target Q-networks
 - 22: **for** $i = 1, 2$ **do**
 - 23: $\zeta_i^{\text{tgt}} \leftarrow \varpi \zeta_i + (1 - \varpi) \zeta_i^{\text{tgt}}$
 - 24: **end for**
 - 25: Compute BC weight:
$$\lambda = \omega \left/ \left\{ \frac{1}{2B} \sum_{\tilde{s} \in \tilde{b}_{\text{src}} \cup b_{\text{tar}}} |\min \{Q_{\zeta_1}(\tilde{s}, \tilde{a}), Q_{\zeta_2}(\tilde{s}, \tilde{a})\}| \right\} \right.$$
 - 26: Compute policy loss gradient:
$$\begin{aligned} \nabla_\varphi \mathcal{L}_\pi \leftarrow & - \frac{\lambda}{|\tilde{b}_{\text{src}} \cup b_{\text{tar}}|} \sum_{\tilde{s} \in \tilde{b}_{\text{src}} \cup b_{\text{tar}}} \nabla_\varphi \left[\min_{i=1,2} Q_{\zeta_i}(\tilde{s}, \tilde{a}) + \alpha \mathcal{H}[\pi_\varphi(\cdot | \tilde{s})] \right] \\ & + \frac{1}{|b_{\text{src}}|} \sum_{(s,a) \in b_{\text{src}}} \nabla_\varphi \|a - \bar{a}\|^2 \end{aligned}$$
 - 27: where $\tilde{a} \sim \pi_\varphi(\cdot | \tilde{s})$, $\bar{a} \sim \pi_\varphi(\cdot | s)$ are independent samples.
 - 28: Update policy: $\varphi \leftarrow \varphi + \text{lr} \nabla_\varphi \mathcal{L}_\pi$
 - 29: **end for**
 - 30: **end for**
 - 31: **Output:** Learned policy π_φ
-

E Proof of Lemma 2.2

Lemma 2.2 (Return Bound between Source Domain and Target Domain [32]). *Let the empirical behavior policy in \mathcal{D}_{src} be $\pi_{\mathcal{D}_{\text{src}}}(a | s)$. Define $C_1 = \frac{2r_{\max}}{(1-\gamma)^2}$. Then for any policy π ,*

$$\begin{aligned} \eta_{\mathcal{M}_{\text{tar}}}(\pi) - \eta_{\mathcal{M}_{\text{src}}}(\pi) &\geq -2C_1 \mathbb{E}_{(s,a) \sim \rho_{\mathcal{M}}^{\pi_{\mathcal{D}_{\text{src}}}, s' \sim p_{\text{src}}}} [D_{\text{TV}}(\pi(\cdot | s') \parallel \pi_{\mathcal{D}_{\text{src}}}(\cdot | s'))] \\ &\quad - C_1 \mathbb{E}_{(s,a) \sim \rho_{\mathcal{M}}^{\pi_{\mathcal{D}_{\text{src}}}}} [D_{\text{TV}}(p_{\text{tar}}(\cdot | s, a) \parallel p_{\text{src}}(\cdot | s, a))]. \end{aligned}$$

Proof. Proof of Lemma 2.2 is already provided as an intermediate step for Theorem A.4 in [32], the offline performance bound case. We include their proof here with slight modifications for completeness.

We first cite the following two necessary lemmas also used in [32]. \square

Lemma E.1 (Extended telescoping lemma). *Denote $\mathcal{M}_1 = (\mathcal{S}, \mathcal{A}, P_1, r, \gamma)$ and $\mathcal{M}_2 = (\mathcal{S}, \mathcal{A}, P_2, r, \gamma)$ as two MDPs that only differ in their transition dynamics. Suppose we have two policies π_1, π_2 , we can reach the following conclusion:*

$$\eta_{\mathcal{M}_1}(\pi_1) - \eta_{\mathcal{M}_2}(\pi_2) = \frac{1}{1-\gamma} \mathbb{E}_{\rho_{\mathcal{M}_1}^{\pi_1}(s,a)} [\mathbb{E}_{s' \sim P_1, a' \sim \pi_1} [Q_{\mathcal{M}_2}^{\pi_2}(s', a')] - \mathbb{E}_{s' \sim P_2, a' \sim \pi_2} [Q_{\mathcal{M}_2}^{\pi_2}(s', a')]].$$

Proof. This is Lemma C.2 in [59]. \square

Lemma E.2. *Denote $\mathcal{M} = (\mathcal{S}, \mathcal{A}, P, r, \gamma)$ as the underlying MDP. Suppose we have two policies π_1, π_2 , then the performance difference of these policies in the MDP gives:*

$$\eta_{\mathcal{M}}(\pi_1) - \eta_{\mathcal{M}}(\pi_2) = \frac{1}{1-\gamma} \mathbb{E}_{\rho_{\mathcal{M}}^{\pi_1}(s,a), s' \sim P} [\mathbb{E}_{a' \sim \pi_1} [Q_{\mathcal{M}}^{\pi_2}(s', a')] - \mathbb{E}_{a' \sim \pi_2} [Q_{\mathcal{M}}^{\pi_2}(s', a')]].$$

Proof. This is Lemma B.3 in [32]. \square

Proof. We have access to the offline source data \mathcal{M}_{src} and the empirical behavioral policy $\pi_{\mathcal{D}_{\text{src}}}$, so we bound the performance between $J_{\mathcal{M}_{\text{tar}}}(\pi)$ and $J_{\mathcal{M}_{\text{src}}}(\pi_{\mathcal{D}_{\text{src}}})$. We have

$$\eta_{\mathcal{M}_{\text{tar}}}(\pi) - \eta_{\pi_{\mathcal{D}_{\text{src}}}}(\pi) = \underbrace{\eta_{\mathcal{M}_{\text{tar}}}(\pi) - \eta_{\mathcal{M}_{\text{src}}}(\pi_{\mathcal{D}_{\text{src}}})}_{(a)} + \underbrace{\eta_{\pi_{\mathcal{D}_{\text{src}}}}(\pi_{\mathcal{D}_{\text{src}}}) - \eta_{\pi_{\mathcal{D}_{\text{src}}}}(\pi)}_{(b)}. \quad (9)$$

To bound (a) term, we use Lemma E.1 in the second equality

$$\begin{aligned} &\eta_{\mathcal{M}_{\text{tar}}}(\pi) - \eta_{\mathcal{M}_{\text{src}}}(\mathcal{D}_{\text{src}}) \\ &= -(\eta_{\mathcal{M}_{\text{src}}}(\mathcal{D}_{\text{src}}) - \eta_{\mathcal{M}_{\text{tar}}}(\pi)) \\ &= -\frac{1}{1-\gamma} \mathbb{E}_{(s,a) \sim \rho_{\mathcal{M}_{\text{src}}}^{\mathcal{D}_{\text{src}}}} [\mathbb{E}_{s'_{\text{src}} \sim p_{\mathcal{M}_{\text{src}}}, a' \sim \pi_{\mathcal{D}_{\text{src}}}} [Q_{\mathcal{M}_{\text{tar}}}^{\pi}(s'_{\text{src}}, a')] - \mathbb{E}_{s'_{\text{tar}} \sim p_{\mathcal{M}_{\text{tar}}}, a' \sim \pi} [Q_{\mathcal{M}_{\text{tar}}}^{\pi}(s'_{\text{tar}}, a')]] \\ &= -\frac{1}{1-\gamma} \mathbb{E}_{(s,a) \sim \rho_{\mathcal{M}_{\text{src}}}^{\mathcal{D}_{\text{src}}}} [\\ &\quad \underbrace{(\mathbb{E}_{s'_{\text{src}} \sim p_{\mathcal{M}_{\text{src}}}, a' \sim \pi_{\mathcal{D}_{\text{src}}}} [Q_{\mathcal{M}_{\text{tar}}}^{\pi}(s'_{\text{src}}, a')] - \mathbb{E}_{s'_{\text{src}} \sim p_{\mathcal{M}_{\text{src}}}, a' \sim \pi} [Q_{\mathcal{M}_{\text{tar}}}^{\pi}(s'_{\text{src}}, a')])}_{(c)} \\ &\quad + \underbrace{(\mathbb{E}_{s'_{\text{src}} \sim p_{\mathcal{M}_{\text{src}}}, a' \sim \pi} [Q_{\mathcal{M}_{\text{tar}}}^{\pi}(s'_{\text{src}}, a')] - \mathbb{E}_{s'_{\text{tar}} \sim p_{\mathcal{M}_{\text{tar}}}, a' \sim \pi} [Q_{\mathcal{M}_{\text{tar}}}^{\pi}(s'_{\text{tar}}, a')])}_{(d)}]. \end{aligned}$$

To bound term (c), we use

$$\begin{aligned} &\mathbb{E}_{s'_{\text{src}} \sim p_{\mathcal{M}_{\text{src}}}, a' \sim \pi_{\mathcal{D}_{\text{src}}}} [Q_{\mathcal{M}_{\text{tar}}}^{\pi}(s'_{\text{src}}, a')] - \mathbb{E}_{s'_{\text{src}} \sim p_{\mathcal{M}_{\text{src}}}, a' \sim \pi} [Q_{\mathcal{M}_{\text{tar}}}^{\pi}(s'_{\text{src}}, a')] \\ &\leq \mathbb{E}_{s'_{\text{src}} \sim p_{\mathcal{M}_{\text{src}}}} \left[\sum_{a' \in \mathcal{A}} |\mathcal{D}_{\text{src}}(a' | s'_{\text{src}}) - \pi(a' | s'_{\text{src}})| \cdot |Q_{\mathcal{M}_{\text{tar}}}^{\pi}(s'_{\text{src}}, a')| \right] \\ &\leq \frac{2r_{\max}}{1-\gamma} \mathbb{E}_{s'_{\text{src}} \sim p_{\mathcal{M}_{\text{src}}}} [D_{\text{TV}}(\pi_{\mathcal{D}_{\text{src}}}(\cdot | s'_{\text{src}}) \parallel \pi(\cdot | s'_{\text{src}}))], \end{aligned}$$

where the last inequality comes from the fact that $|Q_{\mathcal{M}_{\text{tar}}}^\pi(s'_{\text{src}}, a')| \leq \frac{r_{\max}}{1-\gamma}$ and the definition of TV distance.

$$\begin{aligned}
(d) &= \mathbb{E}_{s' \sim p_{\mathcal{M}_{\text{src}}}, a' \sim \pi} [Q_{\mathcal{M}_{\text{tar}}}^\pi(s', a')] - \mathbb{E}_{s' \sim p_{\mathcal{M}_{\text{tar}}}, a' \sim \pi} [Q_{\mathcal{M}_{\text{tar}}}^\pi(s', a')] \\
&= \int_{\mathcal{S}} (p_{\mathcal{M}_{\text{src}}}(s' | s, a) - p_{\mathcal{M}_{\text{tar}}}(s' | s, a)) \left(\sum_{a'} \pi(a' | s') Q_{\mathcal{M}_{\text{tar}}}^\pi(s', a') \right) ds' \\
&\leq \frac{r_{\max}}{1-\gamma} \int_{\mathcal{S}} |p_{\mathcal{M}_{\text{src}}}(s' | s, a) - p_{\mathcal{M}_{\text{tar}}}(s' | s, a)| ds' \\
&= \frac{2r_{\max}}{1-\gamma} [D_{\text{TV}}(p_{\mathcal{M}_{\text{src}}}(\cdot | s, a) \| p_{\mathcal{M}_{\text{tar}}}(\cdot | s, a))],
\end{aligned}$$

where the inequality comes from the fact that $Q_{\mathcal{M}_{\text{tar}}}^\pi(s', a')$ weighted by probability is bounded by $\frac{r_{\max}}{1-\gamma}$, the upper bound for all Q-values.

Combine the bounds for (c) and (d), we obtain a bound for the (a) term:

$$\begin{aligned}
\eta_{\mathcal{M}_{\text{tar}}}(\pi) - \eta_{\mathcal{M}_{\text{src}}}(\pi_{\mathcal{D}_{\text{src}}}) &\geq -\frac{2r_{\max}}{(1-\gamma)^2} \mathbb{E}_{(s,a) \sim \rho_{\mathcal{M}_{\text{src}}}^{\pi_{\mathcal{D}_{\text{src}}}}, s' \sim p_{\mathcal{M}_{\text{src}}}} [D_{\text{TV}}(\pi_{\mathcal{D}_{\text{src}}}(\cdot | s') \| \pi(\cdot | s'))] \\
&\quad - \frac{2r_{\max}}{(1-\gamma)^2} \mathbb{E}_{(s,a) \sim \rho_{\mathcal{M}_{\text{src}}}^{\pi_{\mathcal{D}_{\text{src}}}}} [D_{\text{TV}}(p_{\mathcal{M}_{\text{src}}}(\cdot | s, a) \| p_{\mathcal{M}_{\text{tar}}}(\cdot | s, a))].
\end{aligned}$$

Now we try to bound term (b).

$$\begin{aligned}
&\eta_{\mathcal{M}_{\text{src}}}(\pi_{\mathcal{D}_{\text{src}}}) - \eta_{\mathcal{M}_{\text{src}}}(\pi) \\
&= \frac{1}{1-\gamma} \mathbb{E}_{(s,a) \sim \rho_{\mathcal{M}_{\text{src}}}^{\pi_{\mathcal{D}_{\text{src}}}}, s' \sim p_{\mathcal{M}_{\text{src}}}(\cdot | s, a)} [\mathbb{E}_{a' \sim \pi_{\mathcal{D}_{\text{src}}}} [Q_{\mathcal{M}_{\text{src}}}^\pi(s', a')] - \mathbb{E}_{a' \sim \pi} [Q_{\mathcal{M}_{\text{src}}}^\pi(s', a')]] \\
&\geq -\frac{1}{1-\gamma} \mathbb{E}_{(s,a) \sim \rho_{\mathcal{M}_{\text{src}}}^{\pi_{\mathcal{D}_{\text{src}}}}, s' \sim p_{\mathcal{M}_{\text{src}}}(\cdot | s, a)} |\mathbb{E}_{a' \sim \pi_{\mathcal{D}_{\text{src}}}} [Q_{\mathcal{M}_{\text{src}}}^\pi(s', a')] - \mathbb{E}_{a' \sim \pi} [Q_{\mathcal{M}_{\text{src}}}^\pi(s', a')]| \\
&\geq -\frac{1}{1-\gamma} \mathbb{E}_{(s,a) \sim \rho_{\mathcal{M}_{\text{src}}}^{\pi_{\mathcal{D}_{\text{src}}}}, s' \sim p_{\mathcal{M}_{\text{src}}}(\cdot | s, a)} \left| \sum_{a' \in \mathcal{A}} (\pi_{\mathcal{D}_{\text{src}}}(a' | s') - \pi(a' | s')) Q_{\mathcal{M}_{\text{src}}}^\pi(s', a') \right| \\
&\geq -\frac{r_{\max}}{(1-\gamma)^2} \mathbb{E}_{(s,a) \sim \rho_{\mathcal{M}_{\text{src}}}^{\pi_{\mathcal{D}_{\text{src}}}}, s' \sim p_{\mathcal{M}_{\text{src}}}(\cdot | s, a)} \left| \sum_{a' \in \mathcal{A}} (\pi_{\mathcal{D}_{\text{src}}}(a' | s') - \pi(a' | s')) \right| \\
&= -\frac{2r_{\max}}{(1-\gamma)^2} \mathbb{E}_{(s,a) \sim \rho_{\mathcal{M}_{\text{src}}}^{\pi_{\mathcal{D}_{\text{src}}}}, s' \sim p_{\mathcal{M}_{\text{src}}}(\cdot | s, a)} [D_{\text{TV}}(\pi_{\mathcal{D}_{\text{src}}}(\cdot | s') \| \pi(\cdot | s'))],
\end{aligned}$$

where the first equality is a direct application of Lemma E.2. Combine the bound for term (a) and (b), we conclude that

$$\begin{aligned}
\eta_{\mathcal{M}_{\text{tar}}}(\pi) - \eta_{\mathcal{M}_{\text{src}}}(\pi) &\geq -2C_1 \mathbb{E}_{(s,a) \sim \rho_{\mathcal{M}}^{\pi_{\mathcal{D}_{\text{src}}}}, s' \sim p_{\text{src}}} [D_{\text{TV}}(\pi(\cdot | s') \| \pi_{\mathcal{D}_{\text{src}}}(\cdot | s'))] \\
&\quad - C_1 \mathbb{E}_{(s,a) \sim \rho_{\mathcal{M}}^{\pi_{\mathcal{D}_{\text{src}}}}} [D_{\text{TV}}(p_{\text{tar}}(\cdot | s, a) \| p_{\text{src}}(\cdot | s, a))],
\end{aligned}$$

where $C_1 = \frac{2r_{\max}}{(1-\gamma)^2}$. □

F Proof of Theorem 3.1

Theorem 3.1 (Conditions for Composite Flow Yielding Smaller Errors). *We assume the state space is bounded for both source and target domains, i.e., $|s| \leq \zeta \forall s \in \mathcal{S}$. For an unseen sample pair (s, a) , there exists a constant $C > 0$ (independent of sample sizes and problem dimension) such that, the mean square error of the composite flow Err_{compst} is smaller than that of the direct flow Err_{direct} , i.e., $Err_{\text{compst}} < Err_{\text{direct}}$ whenever the total-variation distance obeys the explicit bound*

$$D_{\text{TV}}(p_{\text{src}}(\cdot | s, a), p_{\text{tar}}(\cdot | s, a)) \leq \frac{C}{\zeta^2} \left(-\frac{\text{Tr}(\Sigma_{s'}^{\text{src}})}{\sqrt{N_{\text{src}}}} + \frac{\text{Tr}(\Sigma_{s'}^{\text{tar}})}{\sqrt{N_{\text{tar}}}} \right) \forall s, a,$$

where $\Sigma_{s'}^{\text{tar}}, \Sigma_{s'}^{\text{src}}$ are the covariance matrices of the N_{tar} samples collected in the target MDP and the N_{src} samples collected in the source MDP, respectively.

Proof. We will use $\nu := \begin{bmatrix} s \\ a \end{bmatrix}$ to denote the state action pair. According to [57], for an estimator \hat{s}' generated by a linear path flow, the squared error admits the bound

$$\|s' - \hat{s}'\|^2 < \text{Tr}(\Sigma_{s'}) - \text{Tr}(\Sigma_{s'\nu}\Sigma_\nu^{-1}\Sigma_{\nu s'}) = \text{Var}(s' | \nu),$$

where $\Sigma_{s'}$, Σ_ν , and $\Sigma_{s'\nu}$ are the covariance and cross-covariance matrices of s' and ν .

Using the N_{tar} target samples to train the direct flow, we have

$$Err_{\text{direct}} = \text{Var}(s' | \nu)_{\text{tar}} + O\left(\frac{\sigma_{\text{tar}}^2}{\sqrt{N_{\text{tar}}}}\right), \quad \sigma_{\text{tar}}^2 := \text{Tr}(\Sigma_{s'}^{\text{tar}}).$$

The composite flow first trains on the N_{src} source samples and then adapts to the target distribution. Standard covariance concentration therefore gives

$$Err_{\text{cmpst}} \leq \text{Var}(s' | \nu)_{\text{src}} + O\left(\frac{\sigma_{\text{src}}^2}{\sqrt{N_{\text{src}}}}\right), \quad \sigma_{\text{src}}^2 := \text{Tr}(\Sigma_{s'}^{\text{src}}).$$

For $Err_{\text{cmpst}} < Err_{\text{direct}}$, a sufficient condition is

$$\text{Var}(s' | \nu)_{\text{src}} - \text{Var}(s' | \nu)_{\text{tar}} < O\left(\frac{\sigma_{\text{tar}}^2}{\sqrt{N_{\text{tar}}}} - \frac{\sigma_{\text{src}}^2}{\sqrt{N_{\text{src}}}}\right). \quad (8)$$

Now we related the variance gap between source and target transitions to total variation distance between source and target transitions. Consider $s' \in \mathbb{R}^d$ be a random vector. Let P, Q be two probability distributions on \mathbb{R}^d , and recall that $|s'| \leq \zeta$.

The variance difference is as follows and we bound it clearly by triangle inequality:

$$|\text{Var}_P(s') - \text{Var}_Q(s')| = |\mathbb{E}_P[s'^2] - (\mathbb{E}_P[s'])^2 - (\mathbb{E}_Q[s'^2] - (\mathbb{E}_Q[s'])^2)| \quad (9)$$

$$= |(\mathbb{E}_P[s'^2] - \mathbb{E}_Q[s'^2]) - [(\mathbb{E}_P[s'])^2 - (\mathbb{E}_Q[s'])^2]| \quad (10)$$

$$\leq |\mathbb{E}_P[s'^2] - \mathbb{E}_Q[s'^2]| + |(\mathbb{E}_P[s'])^2 - (\mathbb{E}_Q[s'])^2|. \quad (11)$$

For the first term:

$$|\mathbb{E}_P[s'^2] - \mathbb{E}_Q[s'^2]| = \left| \int s'^2 (P(s') - Q(s')) ds' \right| \leq \zeta^2 \|P - Q\|_1,$$

since $|s'|^2 \leq \zeta^2$ (bounded state space) and the absolute difference is directly bounded by total variation norm $\|P - Q\|_1$.

For the second term, explicitly factor it:

$$|(\mathbb{E}_P[s'])^2 - (\mathbb{E}_Q[s'])^2| = |\mathbb{E}_P[s'] - \mathbb{E}_Q[s']| \cdot |\mathbb{E}_P[s'] + \mathbb{E}_Q[s']|.$$

Each expectation is bounded by ζ since $|s'| \leq \zeta$:

$$|(\mathbb{E}_P[s'])^2 - (\mathbb{E}_Q[s'])^2| \leq |\mathbb{E}_P[s'] - \mathbb{E}_Q[s']| \cdot 2\zeta.$$

Moreover, explicitly bounding the expectation difference by total variation distance (standard property of expectations w.r.t. total variation):

$$|\mathbb{E}_P[s'] - \mathbb{E}_Q[s']| = \left| \int s' \cdot (P(s') - Q(s')) ds' \right| \leq \zeta \|P - Q\|_1.$$

Thus rigorously, the second term is bounded as:

$$|(\mathbb{E}_P[s'])^2 - (\mathbb{E}_Q[s'])^2| \leq 2\zeta^2 \|P - Q\|_1.$$

Combining both terms explicitly yields:

$$|\text{Var}_P(s') - \text{Var}_Q(s')| \leq 3\zeta^2 \|P - Q\|_1$$

Applying this with $P = p_{\text{src}}(\cdot | \nu)$ and $Q = p_{\text{tar}}(\cdot | \nu)$ and taking the supremum over ν gives

$$\text{Var}(s' | \nu)_{\text{src}} - \text{Var}(s' | \nu)_{\text{tar}} \leq 3\zeta^2 \sup_{\nu} D_{\text{TV}}(p_{\text{src}}(\cdot | \nu), p_{\text{tar}}(\cdot | \nu)).$$

We thus get a sufficient condition for the composite flow to outperform the direct flow is

$$3\zeta^2 \sup_{\nu} D_{\text{TV}}(p_{\text{src}}(\cdot | \nu), p_{\text{tar}}(\cdot | \nu)) < O\left(\frac{\sigma_{\text{tar}}^2}{\sqrt{N_{\text{tar}}}} - \frac{\sigma_{\text{src}}^2}{\sqrt{N_{\text{src}}}}\right),$$

or, equivalently,

$$D_{\text{TV}}(p_{\text{src}}, p_{\text{tar}}) = O\left(\frac{1}{\zeta^2} \left(\frac{\text{Tr}(\Sigma_{s'}^{\text{tar}})}{\sqrt{N_{\text{tar}}}} - \frac{\text{Tr}(\Sigma_{s'}^{\text{src}})}{\sqrt{N_{\text{src}}}}\right)\right),$$

which is precisely the condition stated in the theorem. \square

G Proof of Theorem 3.3

To prove theorem 3.3, we first prove the following lemma which bounds the Wasserstein-2 distance estimation error of the optimal transport flow matching model by the square root of its mean square error.

Lemma G.1 (Wasserstein-2 Distance Estimation Bound). *Let $p_{\text{src}}, p_{\text{tar}} \in \mathcal{P}_2(\mathbb{R}^d)$ be source and target distributions that also satisfies assumptions (A1) and (A2) in Proposition 3.2 (see Appendix H). Let $\hat{T} : \mathbb{R}^d \rightarrow \mathbb{R}^d$ be a learned transport map obtained by flow matching, and define the pushforward distribution $\hat{p}_{\text{tar}} := \hat{T}_{\#} p_{\text{src}}$. Then the error in estimating the Wasserstein-2 distance between the source and target distributions using \hat{T} is bounded by the square root of the mean squared error between $\hat{T}(x_0)$ and the true matched target sample s , i.e.,*

$$|W_2(p_{\text{src}}, p_{\text{tar}}) - W_2(p_{\text{src}}, \hat{p}_{\text{tar}})| \leq \sqrt{\text{ErrMSE}}.$$

Proof. Note that $W_2(\cdot, \cdot)$ is a metric, so by the triangle inequality, we have:

$$|W_2(p_{\text{src}}, p_{\text{tar}}) - W_2(p_{\text{src}}, \hat{p}_{\text{tar}})| \leq W_2(p_{\text{tar}}, \hat{p}_{\text{tar}}).$$

Because assumptions (A1) and (A2) in Proposition 3.2 are satisfied, by Brenier theorem there exists a deterministic optimal transport map T . We denote a sample from the source distribution x_0 and the matching target sample induced by the true optimal transport map T as $s := T(x_0)$, and the matching target sample induced by the learned optimal transport map \hat{T} as $\hat{s} := \hat{T}(x_0)$.

We consider $(x_0, s) \sim q$, where q is a coupling between the real source and target distributions used in training the flow matching model, with marginals $x_0 \sim p_{\text{src}}$ and $s \sim p_{\text{tar}}$. Let $\Pi(\hat{p}_{\text{tar}}, p_{\text{tar}})$ denote the set of all couplings between \hat{p}_{tar} and p_{tar} . By the definition of W_2 , we have:

$$W_2^2(p_{\text{tar}}, \hat{p}_{\text{tar}}) = \inf_{q' \in \Pi(p_{\text{tar}}, \hat{p}_{\text{tar}})} \mathbb{E}_{(\hat{s}, s) \sim q'} \|\hat{s} - s\|^2 \leq \mathbb{E}_{(x_0, s) \sim q} \|\hat{T}(x_0) - s\|^2$$

So:

$$W_2(p_{\text{tar}}, \hat{p}_{\text{tar}}) \leq \sqrt{\mathbb{E}_{(x_0, s) \sim q} \|\hat{T}(x_0) - s\|^2} = \sqrt{\text{ErrMSE}}$$

This completes the proof. \square

Theorem 3.3 (Large Dynamics Gap Exploration Reduces Performance Gap). *Compared to behavior cloning on the offline source dataset, training a policy $\hat{\pi}$ by replacing all source samples with a dynamics gap exceeding κ (as estimated by the composite flow) with target domain samples can reduce the performance gap to the optimal target policy π_{tar}^* by*

$$\Delta_{\kappa} = \frac{4L_r(1+\gamma)}{(1-\gamma)(1-\gamma L_p)} \left(\Delta_{W_2} - \kappa - \sqrt{\text{Var}(s' | \nu)_{\text{tar}} + O\left(\frac{\text{Tr}(\Sigma_{s'}^{\text{tar}})}{\sqrt{N_{\text{tar}}}}\right)} \right) \quad (5)$$

Here L_r and L_p are the Lipschitz constants for the reward and transition function, respectively. $\gamma L_p < 1$. $\Delta_{W_2} := \sup_{s,a} W_2(p_{\text{src}}(\cdot | s, a), p_{\text{tar}}(\cdot | s, a))$ is the largest dynamics gap. $\text{Var}(s' | s, a)_{\text{tar}}$ is the conditional variance of s' given s, a under the distribution p_{tar} .

Proof. We list the full description of assumptions made in the theorem statement:

1. Lipschitz reward. For every $a \in \mathcal{A}$ the map $s \mapsto r(s, a)$ is L_r -Lipschitz:

$$|r(s, a) - r(s', a)| \leq L_r d(s, s') \quad \forall s, s', a.$$

2. Lipschitz dynamics. Both kernels are L_p -Lipschitz in Wasserstein distance:

$$W_1(p_m(\cdot | s, a), p_m(\cdot | s', a)) \leq L_p d(s, s') \quad \forall s, s', a, m \in \{\text{src}, \text{tar}\}.$$

3. Contraction margin. $\gamma L_p < 1$.

Let's first study the performance of a policy π trained with the source MDP dataset on the target MDP $\eta_{\mathcal{M}_{\text{tar}}}(\pi)$. Denote $\Delta_{W_1} := \sup_{s, a} W_1(p_{\text{src}}(\cdot | s, a), p_{\text{tar}}(\cdot | s, a))$.

Given a fixed policy π , we cite Theorem 3.1 in [40] for the following bound:

$$\begin{aligned} \|V_{\text{tar}}^\pi - V_{\text{src}}^\pi\|_\infty &\leq 2L_r \Delta_{W_1} (1 + \gamma) \sum_{i=0}^{\infty} \gamma^i \sum_{j=0}^i (L_P)^j \\ &= 2L_r \Delta_{W_1} (1 + \gamma) \sum_{j=0}^{\infty} (L_P)^j \sum_{i=j}^{\infty} \gamma^i \\ &= 2L_r \Delta_{W_1} (1 + \gamma) \sum_{j=0}^{\infty} (L_P)^j \cdot \frac{\gamma^j}{1 - \gamma} \\ &= \frac{2L_r \Delta_{W_1} (1 + \gamma)}{1 - \gamma} \sum_{j=0}^{\infty} (\gamma L_P)^j \\ &= \frac{2L_r \Delta_{W_1} (1 + \gamma)}{(1 - \gamma)(1 - \gamma L_P)} \end{aligned} \tag{12}$$

Averaging over the initial state-distribution μ gives us a bound on what we call the model gap:

$$\begin{aligned} |\eta_{\mathcal{M}_{\text{tar}}}(\pi) - \eta_{\mathcal{M}_{\text{src}}}(\pi)| &= \left| \int_{\mathcal{S}} (V_{\text{tar}}^\pi(s) - V_{\text{src}}^\pi(s)) \mu(ds) \right| \\ &\leq \int_{\mathcal{S}} |V_{\text{tar}}^\pi(s) - V_{\text{src}}^\pi(s)| \mu(ds) \\ &\leq \|V_{\text{tar}}^\pi - V_{\text{src}}^\pi\|_\infty \\ &\leq \frac{2L_r \Delta_{W_1} (1 + \gamma)}{(1 - \gamma)(1 - \gamma L_P)}. \end{aligned}$$

Moreover, the bounded state space assumption in Theorem 3.1 implies bounded second moment for both p_{src} and p_{tar} , so we have $W_1(p_{\text{src}}, p_{\text{tar}}) \leq W_2(p_{\text{src}}, p_{\text{tar}}) \forall p_{\text{src}}, p_{\text{tar}}$. Hence, we obtain that

$$|\eta_{\mathcal{M}_{\text{tar}}}(\pi) - \eta_{\mathcal{M}_{\text{src}}}(\pi)| \leq \frac{2L_r(1 + \gamma)}{(1 - \gamma)(1 - \gamma L_P)} \Delta_{W_1} \tag{13}$$

$$\leq \frac{2L_r(1 + \gamma)}{(1 - \gamma)(1 - \gamma L_P)} \Delta_{W_2}. \tag{14}$$

For the policy π , we then decompose the performance gap

$$\begin{aligned} &\underbrace{\eta_{\mathcal{M}_{\text{tar}}}(\pi_{\text{tar}}^*) - \eta_{\mathcal{M}_{\text{tar}}}(\pi)}_{\text{desired gap}} \\ &= \underbrace{[\eta_{\mathcal{M}_{\text{tar}}}(\pi_{\text{tar}}^*) - \eta_{\mathcal{M}_{\text{src}}}(\pi_{\text{tar}}^*)]}_{\text{model gap (a)}} + \underbrace{[\eta_{\mathcal{M}_{\text{src}}}(\pi_{\text{tar}}^*) - \eta_{\mathcal{M}_{\text{src}}}(\pi)]}_{\text{learning gap (b)}} + \underbrace{[\eta_{\mathcal{M}_{\text{src}}}(\pi) - \eta_{\mathcal{M}_{\text{tar}}}(\pi)]}_{\text{model gap (c)}}. \end{aligned} \tag{15}$$

Let's call the behavior cloning policy on the offline source dataset π_{bc} , and we use $\varepsilon_{bc} := \eta_{\mathcal{M}_{src}}(\pi_{tar}^*) - \eta_{\mathcal{M}_{src}}(\pi_{bc})$ to denote the learning gap, i.e., the (b) term in decomposition 15.

$$\eta_{\mathcal{M}_{tar}}(\pi_{tar}^*) - \eta_{\mathcal{M}_{tar}}(\hat{\pi}_{bc}) \leq \frac{4L_r(1+\gamma)}{(1-\gamma)(1-\gamma L_p)} \Delta_{W_2} + \varepsilon_{bc}. \quad (16)$$

During the online learning stage, we collect samples with large dynamics gap. Suppose in our policy $\hat{\pi}$, we have all samples with $\Delta_{W_2} > \kappa$ being replaced with samples from the target MDP. Considering MSE errors introduced by flow matching, as in the proof of Theorem 3.1, the errors could be

$$Err_{\kappa} \leq \text{Var}(s'|\nu)_{tar} + O\left(\frac{\sigma_{tar}^2}{\sqrt{N_{tar}}}\right) \quad (17)$$

We denote the source and target distribution of flow matching by p_{src} and p_{tar} , and the pushforward distribution generated by flow matching as \hat{p}_{tar} . By Lemma G.1, we can bound the Wasserstein-2 distance estimation error by

$$|W_2(p_{src}, p_{tar}) - W_2(p_{src}, \hat{p}_{tar})| \leq \sqrt{Err_{\kappa}}$$

Let's use $\varepsilon_N := \eta_{\mathcal{M}_{src}}(\pi_{tar}^*) - \eta_{\mathcal{M}_{src}}(\hat{\pi})$ to denote the learning gap of the fine-tuned policy $\hat{\pi}$ in decomposition 15. Therefore, the performance gap of $\hat{\pi}$ is:

$$\begin{aligned} & \eta_{\mathcal{M}_{tar}}(\pi_{tar}^*) - \eta_{\mathcal{M}_{tar}}(\hat{\pi}) \\ & \leq \frac{4L_r(1+\gamma)}{(1-\gamma)(1-\gamma L_p)} \left(\kappa + \sqrt{\text{Var}(s'|\nu)_{tar} + O\left(\frac{\sigma_{tar}^2}{\sqrt{N_{tar}}}\right)} \right) + \varepsilon_N. \end{aligned} \quad (18)$$

We assume that the model has been trained for sufficiently long time and the network capacity is sufficient so ε_N and ε_{bc} are small and have negligible influences. Therefore, by subtracting RHS of Equation 18 from RHS of Equation 16, we obtain the performance gap reduces at least by

$$\frac{4L_r(1+\gamma)}{(1-\gamma)(1-\gamma L_p)} \left(\Delta_{W_2} - \kappa - \sqrt{\text{Var}(s'|\nu)_{tar} + O\left(\frac{\sigma_{tar}^2}{\sqrt{N_{tar}}}\right)} \right). \quad (19)$$

□

H Proof of Proposition 3.2

We provide the formal version of Proposition 3.2 as below.

Proposition H.1 (Shared-Latent Coupling Approximates W_2 -Optimal Transport). We first introduce some notations for simplicity:

Notation. Fix a state-action pair $(s, a) \in \mathcal{S} \times \mathcal{A}$, and omit (s, a) in the following for notational simplicity. Let the latent distribution be $p_0(x_0) = \mathcal{N}(0, \mathbf{I})$. Define the source transition distribution as $p_1(x_1) := p_{src}(s'|s, a)$, and the target transition distribution as $p_2(x_2) := p_{tar}(s'|s, a)$.

We denote the pretrained source flow $\psi_{\theta}(x, t|s, a)$ by $\psi_{\theta}(x, t)$, and similarly write the target flow $\psi_{\phi}(x, t|s, a)$ as $\psi_{\phi}(x, t)$. Let $\psi_{\phi}^k(x, t)$ denote the target flow model trained on a batch of size k from the target domain.

Assumptions.

(A1) The distributions p_1 and p_2 have bounded support: there exists $C > 0$ such that $\|x\| \leq C$ for all $x \in \text{supp}(p_1) \cup \text{supp}(p_2)$.

(A2) The distribution p_1 admits a density, and the optimal transport map between p_1 and p_2 under the quadratic cost is continuous.

(A3) At each training iteration, we compute the optimal transport plan for the current minibatch.

Dataset	Task Name	BC-SAC	H2O	BC-VGDF	BC-PAR	Ours
MR	Walker2D (Kinematic)	2973 ± 185	1967 ± 851	1586 ± 923	948 ± 131	1568 ± 1315
MR	Halfcheetah (Friction)	7799 ± 157	6397 ± 673	7829 ± 821	8056 ± 512	8241 ± 180
MR	Hopper (Friction)	228 ± 2	229 ± 1	230 ± 3	232 ± 5	280 ± 27
MR	Walker2D (Friction)	311 ± 5	296 ± 14	302 ± 12	321 ± 26	344 ± 20
M	Walker2D (Kinematic)	1966 ± 1155	1965 ± 568	1921 ± 928	806 ± 278	2039 ± 936
M	Halfcheetah (Friction)	7108 ± 1001	6968 ± 846	6802 ± 956	7800 ± 525	7871 ± 238
M	Hopper (Friction)	232 ± 1	228 ± 4	229 ± 4	233 ± 5	300 ± 66
M	Walker2D (Friction)	286 ± 54	298 ± 45	289 ± 47	308 ± 24	320 ± 31
ME	Walker2D (Kinematic)	850 ± 953	1514 ± 782	1204 ± 734	755 ± 268	1511 ± 1206
ME	Halfcheetah (Friction)	4185 ± 732	2140 ± 733	4078 ± 1032	4989 ± 500	5596 ± 1557
ME	Hopper (Friction)	230 ± 3	232 ± 5	230 ± 6	232 ± 8	266 ± 70
ME	Walker2D (Friction)	240 ± 114	258 ± 8	245 ± 51	242 ± 24	326 ± 26
Average Return		2201	1874	2079	2077	2389

Table 2: Comparison of policy performance across frictional and kinematic dynamics shifts under three dataset regimes: MR = Medium Replay, M = Medium, ME = Medium Expert. Green highlights indicate the top-performing method with $\geq 2\%$ improvement; yellow indicates ties within 2%.

Result. Let $W_2^2(p_1, p_2)$ denote the squared 2-Wasserstein distance between p_1 and p_2 , defined as

$$W_2^2(p_1, p_2) := \min_{q \in \Pi(p_1, p_2)} \mathbb{E}_{(x_1, x_2) \sim q} [\|x_2 - x_1\|_2^2],$$

where $\Pi(p_1, p_2)$ denotes the set of all couplings (i.e., joint distributions) with marginals p_1 and p_2 .

Then, in the limit as $\eta \rightarrow \infty$ (in the cost function of Algorithm 3) and $k \rightarrow \infty$, we have

$$\lim_{k \rightarrow \infty} \mathbb{E}_{x_0 \sim \mathcal{N}(0, \mathbf{I})} [\|\psi_\theta(x_0, 1) - \psi_\phi^k(\psi_\theta(x_0, 1), 2)\|^2] = W_2^2(p_1, p_2),$$

where ψ_θ denotes the source flow and ψ_ϕ^k is the target flow trained on a batch of size k .

Proof. We begin by reparameterizing the expectation using the definition of the pushforward distribution induced by the source flow, $p_1 = \psi_\theta(x, 1) \# p_0$. Specifically,

$$\lim_{k \rightarrow \infty} \mathbb{E}_{x_0 \sim p_0} [\|\psi_\theta(x_0, 1) - \psi_\phi^k(\psi_\theta(x_0, 1), 2)\|^2] = \lim_{k \rightarrow \infty} \mathbb{E}_{x_1 \sim p_1} [\|x_1 - \psi_\phi^k(x_1, 2)\|^2].$$

According to Proposition 3.1 in [17], as $\eta \rightarrow \infty$, mass transport in the conditional variables (s, a) vanishes. That is, the transport is concentrated exclusively in the next-state space, and optimal transport is performed independently within each fixed (s, a) pair when $\eta \rightarrow \infty$.

Therefore, for any fixed (s, a), we can invoke Theorem 4.2 from [42], which guarantees that the expected transport cost under the batch-trained flow ψ_ϕ^k converges to the squared 2-Wasserstein distance between p_1 and p_2 as the batch size $k \rightarrow \infty$. Hence,

$$\lim_{k \rightarrow \infty} \mathbb{E}_{x_1 \sim p_1} [\|x_1 - \psi_\phi^k(x_1, 2)\|^2] = W_2^2(p_1, p_2),$$

which concludes the proof. \square

I Additional Experimental Results

I.1 Additional Main Results

We provide additional results on the Walker2D Kinematic and Frictional shift tasks in Table 2. Across these 12 additional tasks, COMPFLOW consistently outperforms other methods—achieving the best performance on 10 tasks, tying on 2, and losing on only 1.

J Experimental Details

In this section, we describe the detailed experimental setup as well as the hyperparameter setup used in this work.

J.1 Environment Setting

J.1.1 Source Domain Dataset

We use the MuJoCo datasets from D4RL [16] as our source domain data. These datasets are collected from continuous control environments in Gym [4], simulated using the MuJoCo physics engine [56]. We focus on three benchmark tasks: *HalfCheetah*, *Hopper*, and *Walker2d*, and evaluate across three dataset types: *medium*, *medium-replay*, and *medium-expert*.

- The *medium* datasets consist of trajectories generated by an SAC policy trained for 1M steps and then early stopped.
- The *medium-replay* datasets capture the replay buffer of a policy trained to the performance level of the medium agent.
- The *medium-expert* datasets are formed by mixing equal proportions of medium and expert data (50-50).

J.1.2 Kinematic Shift Tasks

We use Kinematic Shift Tasks from the benchmark [33]. We select most shift level 'hard' to make the tasks more challenging

- **HalfCheetah Kinematic Shift:** The rotation range of the foot joint is modified to be:

```
<joint axis="0 1 0" damping="3" name="bfoot" pos="0 0 0" range="-.08 .157" stiffness="120" type="hinge"/>
<joint axis="0 1 0" damping="1.5" name="ffoot" pos="0 0 0" range="-.1 .1" stiffness="60" type="hinge"/>
```

- **Hopper Kinematic Shift:** the rotation range of the foot joint is modified from $[-45, 45]$ to $[-9, 9]$:

```
<joint axis="0 -1 0" name="foot_joint" pos="0 0 0.1" range="-9 9" type="hinge"/>
```

- **Walker2D Kinematic Shift:** the rotation range of the foot joint is modified from $[-45, 45]$ to $[-9, 9]$:

```
<joint axis="0 -1 0" name="foot_joint" pos="0 0 0.1" range="-9 9" type="hinge"/>
<joint axis="0 -1 0" name="foot_left_joint" pos="0 0 0.1" range="-9 9" type="hinge" />
```

J.1.3 Morphology Shift Tasks

We use Morphology Shift Tasks from the benchmark [33]. We select most shift level 'hard' to make the tasks more challenging

- **HalfCheetah Morphology Shift:** the front thigh size and the back thigh size are modified to be:

```
<geom fromto="0 0 0.02 0 -0.02" name="bthigh" size="0.046" type="capsule"/>
<body name="fshin" pos="0.02 0 -0.02">
  <geom fromto="0 0 0 -.13 0 -.15" name="bshin" rgba="0.9 0.6 0.6 1" size="0.046" type="capsule"/>
</body>
<body name="bfoot" pos="-.13 0 -.15">
  <geom fromto="0 0 0 -.04 0 -0.05" name="fthigh" size="0.046" type="capsule"/>
</body>
<body name="fshin" pos="0 -.04 0 -0.05">
  <geom fromto="0 0 0 .11 0 -.13" name="fshin" rgba="0.9 0.6 0.6 1" size="0.046" type="capsule"/>
</body>
<body name="ffoot" pos=".11 0 -.13"/>
```

- **Hopper Morphology Shift:** the foot size is revised to be 0.4 times of that within the source domain:

```
<geom friction="2.0" fromto="-0.052 0 0.1 0.104 0 0.1" name="foot_geom" size="0.024" type="capsule"/>
```

- **Walker2D Morphology Shift:** the leg size of the robot is revised to be 0.2 times of that in the source domain.

```

<geom friction="0.9" fromto="0 0 1.05 0 0 0.2" name="thigh_geom" size="0.05" type="
capsule"/>
<joint axis="0 -1 0" name="leg_joint" pos="0 0 0.2" range="-150 0" type="hinge"/>
<geom friction="0.9" fromto="0 0 0.2 0 0 0.1" name="leg_geom" size="0.04" type="
capsule"/>
<geom friction="0.9" fromto="0 0 1.05 0 0 0.2" name="thigh_left_geom" rgba=".7 .3 .6
1" size="0.05" type="capsule"/>
<joint axis="0 -1 0" name="leg_left_joint" pos="0 0 0.2" range="-150 0" type="hinge"
/>
<geom friction="0.9" fromto="0 0 0.2 0 0 0.1" name="leg_left_geom" rgba=".7 .3 .6 1"
size="0.04" type="capsule"/>

```

J.1.4 Friction Shift Tasks

Following [33], the friction shift is implemented by altering the friction attribute in the geom elements. The frictional components are adjusted to 5.0 times the frictional components in the source domain. The following is an example for the Hopper robot.

Listing 1: Geometry Definitions for Walker2D

```

# torso
<geom friction="4.5" fromto="0 0 1.45 0 0 1.05" name="torso_geom" size="0.05" type="
capsule"/>
# thigh
<geom friction="4.5" fromto="0 0 1.05 0 0 0.6" name="thigh_geom" size="0.05" type="
capsule"/>
# leg
<geom friction="4.5" fromto="0 0 0.6 0 0 0.1" name="leg_geom" size="0.04" type="
capsule"/>
# foot
<geom friction="10.0" fromto="-0.13 0 0.1 0.26 0 0.1" name="foot_geom" size="0.06"
type="capsule"/>

```

J.2 Implementation Details

BC-SAC: This baseline leverages both offline source domain data and online target domain transitions for policy learning. Since learning from offline data requires conservatism while online data does not, we incorporate a behavior cloning term into the actor update of the SAC algorithm. Specifically, the critic is updated using standard Bellman loss on the combined offline and online datasets, and the actor is optimized as:

$$\mathcal{L}_{\text{actor}} = \lambda \cdot \mathbb{E}_{s \sim \mathcal{D}_{\text{src}} \cup \mathcal{D}_{\text{tar}}, a \sim \pi_{\varphi}(\cdot|s)} \left[\min_{i=1,2} Q_{\zeta_i}(s, a) - \alpha \log \pi_{\varphi}(\cdot|s) \right] + \mathbb{E}_{(s,a) \sim \mathcal{D}_{\text{src}}, \hat{a} \sim \pi_{\varphi}(\cdot|s)} [(a - \hat{a})^2], \quad (20)$$

where $\lambda = \frac{\omega}{\frac{1}{N} \sum_{(s_j, a_j)} \min_{i=1,2} Q_{\zeta_i}(s_j, a_j)}$ and $\omega \in \mathbb{R}^+$ is a normalization coefficient. We train BC-SAC for 400K gradient steps, collecting target domain data every 10 steps. We use the hyperparameters recommended in [33].

H2O: H2O [41] trains domain classifiers to estimate dynamics gaps and uses them as importance sampling weights during critic training. It also incorporates a CQL loss to encourage conservatism. Since the original H2O is designed for the Online-Offline setting (online source, offline target), we adapt the objective to the Offline-Online setting. The critic loss is:

$$\mathcal{L}_{\text{critic}} = \mathbb{E}_{\mathcal{D}_{\text{tar}}} [(Q_{\zeta_i}(s, a) - y)^2] + \mathbb{E}_{\mathcal{D}_{\text{src}}} [\omega(s, a, s')(Q_{\zeta_i}(s, a) - y)^2] + \beta_{\text{CQL}} (\mathbb{E}_{s \sim \mathcal{D}_{\text{src}}, \hat{a} \sim \pi_{\varphi}(\cdot|s)} [\omega(s, a, s') Q_{\zeta_i}(s, \hat{a})] - \mathbb{E}_{\mathcal{D}_{\text{src}}} [\omega(s, a, s') Q_{\zeta_i}(s, a)]), \quad i \in \{1, 2\}, \quad (21)$$

where $\omega(s, a, s')$ is the dynamics-based importance weight, and β_{CQL} is the penalty coefficient. We set $\beta_{\text{CQL}} = 10.0$, which performs better than the default 0.01. We reproduce H2O using the official

codebase,² and adopt the suggested hyperparameters. H2O is trained for 40K environment steps, with 10 gradient updates per step.

BC-VGDF: BC-VGDF [59] filters source transitions whose estimated values align closely with those from the target domain. It trains an ensemble of dynamics models to predict next states from raw state-action pairs under the target dynamics. Each predicted next state is evaluated by the policy to obtain a value ensemble $\{Q(s'_i, a'_i)\}_{i=1}^M$, forming a Gaussian distribution. A fixed percentage ($\xi\%$) of source transitions with the highest likelihood under this distribution are retained. The critic loss is:

$$\begin{aligned} \mathcal{L}_{\text{critic}} = & \mathbb{E}_{(s,a,r,s') \sim \mathcal{D}_{\text{tar}}} \left[(Q_{\zeta_i}(s, a) - y)^2 \right] \\ & + \mathbb{E}_{(s,a,r,s') \sim \mathcal{D}_{\text{src}}} \left[\mathbf{1}(\Lambda(s, a, s') > \Lambda_{\xi\%}) (Q_{\zeta_i}(s, a) - y)^2 \right], \quad i \in \{1, 2\}, \end{aligned} \quad (22)$$

where $\Lambda(s, a, s')$ denotes the fictitious value proximity (FVP), and $\Lambda_{\xi\%}$ is the ξ -quantile threshold. VGDF also trains an exploration policy. Actor training includes a behavior cloning term, as in BC-SAC. We follow the official implementation,³ use the recommended hyperparameters, and train for 40K environment steps with 10 gradient updates per step.

BC-PAR: BC-PAR [32] addresses dynamics mismatch through representation mismatch, measured as the deviation between the encoded source state-action pair and its next state. It employs a state encoder f_ψ and a state-action encoder g_ξ , both trained on the target domain. The encoder loss is:

$$\mathcal{L}(\psi, \xi) = \mathbb{E}_{(s,a,s') \sim \mathcal{D}_{\text{tar}}} \left[(g_\xi(f_\psi(s), a) - \text{SG}(f_\psi(s')))^2 \right], \quad (23)$$

where SG is the stop-gradient operator. Source rewards are adjusted as:

$$\hat{r}_{\text{PAR}} = r_{\text{src}} - \beta \cdot \|g_\xi(f_\psi(s_{\text{src}}), a_{\text{src}}) - f_\psi(s'_{\text{src}})\|^2, \quad (24)$$

where β controls the penalty strength. The actor (π_φ) and critic (Q_{ζ_i}) are jointly trained using both source and target data. Actor training includes a behavior cloning term, similar to BC-SAC. We implement BC-PAR using the official codebase,⁴ adopt the suggested hyperparameters, and train for 40K environment steps with 10 gradient updates per step.

COMPFLOW. When training the target flow, we use a quadratic cost function and employ the Python Optimal Transport (POT) library [15] to compute the optimal transport plan for each minibatch using the exact solver. Additional hyperparameters are provided in Table 3 and Table 4. Since the exploration bonus term is closely tied to properties of the environment—such as the state space, action space, and reward structure—it is expected that the optimal exploration strength β varies across tasks. We perform a sweep over $\beta \in \{0.01, 0.1, 0.2\}$, and select the source data selection ratio $\xi\%$ from $\{30\%, 50\%\}$.

²<https://github.com/t6-thu/H2O>

³<https://github.com/Kavka1/VGDF>

⁴<https://github.com/dmksjfl/PAR>

Hyperparameter	Value
Actor network architecture	(256, 256)
Critic network architecture	(256, 256)
Batch size	128
Learning rate	3×10^{-4}
Optimizer	Adam [24]
Discount factor (γ)	0.99
Replay buffer size	10^6
Warmup steps	10^5
Activation	ReLU
Target update rate	5×10^{-3}
SAC temperature coefficient (α)	0.2
Maximum log standard deviation	2
Minimum log standard deviation	-20
Normalization coefficient (ω)	5

Table 3: Hyperparameters for RL training.

Hyperparameter	Source Flow	Target Flow
Number of hidden layers	6	6
Hidden dimension	256	256
Activation	ReLU	ReLU
Batch size	1024	1024
ODE solver method	Euler	Euler
ODE solver steps	10	10
Training frequency	—	5000
Optimizer	Adam	Adam

Table 4: Hyperparameter setup for source and target domain flows

NeurIPS Paper Checklist

1. Claims

Question: Do the main claims made in the abstract and introduction accurately reflect the paper’s contributions and scope?

Answer: [\[Yes\]](#)

Justification: We propose a new method for reinforcement learning with shifted-dynamics data based on flow matching.

Guidelines:

- The answer NA means that the abstract and introduction do not include the claims made in the paper.
- The abstract and/or introduction should clearly state the claims made, including the contributions made in the paper and important assumptions and limitations. A No or NA answer to this question will not be perceived well by the reviewers.
- The claims made should match theoretical and experimental results, and reflect how much the results can be expected to generalize to other settings.
- It is fine to include aspirational goals as motivation as long as it is clear that these goals are not attained by the paper.

2. Limitations

Question: Does the paper discuss the limitations of the work performed by the authors?

Answer: [\[Yes\]](#)

Justification: We discuss the limitations of our method in Section 6.

Guidelines:

- The answer NA means that the paper has no limitation while the answer No means that the paper has limitations, but those are not discussed in the paper.
- The authors are encouraged to create a separate "Limitations" section in their paper.

- The paper should point out any strong assumptions and how robust the results are to violations of these assumptions (e.g., independence assumptions, noiseless settings, model well-specification, asymptotic approximations only holding locally). The authors should reflect on how these assumptions might be violated in practice and what the implications would be.
- The authors should reflect on the scope of the claims made, e.g., if the approach was only tested on a few datasets or with a few runs. In general, empirical results often depend on implicit assumptions, which should be articulated.
- The authors should reflect on the factors that influence the performance of the approach. For example, a facial recognition algorithm may perform poorly when image resolution is low or images are taken in low lighting. Or a speech-to-text system might not be used reliably to provide closed captions for online lectures because it fails to handle technical jargon.
- The authors should discuss the computational efficiency of the proposed algorithms and how they scale with dataset size.
- If applicable, the authors should discuss possible limitations of their approach to address problems of privacy and fairness.
- While the authors might fear that complete honesty about limitations might be used by reviewers as grounds for rejection, a worse outcome might be that reviewers discover limitations that aren't acknowledged in the paper. The authors should use their best judgment and recognize that individual actions in favor of transparency play an important role in developing norms that preserve the integrity of the community. Reviewers will be specifically instructed to not penalize honesty concerning limitations.

3. Theory assumptions and proofs

Question: For each theoretical result, does the paper provide the full set of assumptions and a complete (and correct) proof?

Answer: [Yes]

Justification: We provide all proofs for the theorems, propositions, and lemmas in the Appendix.

Guidelines:

- The answer NA means that the paper does not include theoretical results.
- All the theorems, formulas, and proofs in the paper should be numbered and cross-referenced.
- All assumptions should be clearly stated or referenced in the statement of any theorems.
- The proofs can either appear in the main paper or the supplemental material, but if they appear in the supplemental material, the authors are encouraged to provide a short proof sketch to provide intuition.
- Inversely, any informal proof provided in the core of the paper should be complemented by formal proofs provided in appendix or supplemental material.
- Theorems and Lemmas that the proof relies upon should be properly referenced.

4. Experimental result reproducibility

Question: Does the paper fully disclose all the information needed to reproduce the main experimental results of the paper to the extent that it affects the main claims and/or conclusions of the paper (regardless of whether the code and data are provided or not)?

Answer: [Yes]

Justification: We provide all the experimental details in Appendix J.

Guidelines:

- The answer NA means that the paper does not include experiments.
- If the paper includes experiments, a No answer to this question will not be perceived well by the reviewers: Making the paper reproducible is important, regardless of whether the code and data are provided or not.
- If the contribution is a dataset and/or model, the authors should describe the steps taken to make their results reproducible or verifiable.
- Depending on the contribution, reproducibility can be accomplished in various ways. For example, if the contribution is a novel architecture, describing the architecture fully

might suffice, or if the contribution is a specific model and empirical evaluation, it may be necessary to either make it possible for others to replicate the model with the same dataset, or provide access to the model. In general, releasing code and data is often one good way to accomplish this, but reproducibility can also be provided via detailed instructions for how to replicate the results, access to a hosted model (e.g., in the case of a large language model), releasing of a model checkpoint, or other means that are appropriate to the research performed.

- While NeurIPS does not require releasing code, the conference does require all submissions to provide some reasonable avenue for reproducibility, which may depend on the nature of the contribution. For example
 - (a) If the contribution is primarily a new algorithm, the paper should make it clear how to reproduce that algorithm.
 - (b) If the contribution is primarily a new model architecture, the paper should describe the architecture clearly and fully.
 - (c) If the contribution is a new model (e.g., a large language model), then there should either be a way to access this model for reproducing the results or a way to reproduce the model (e.g., with an open-source dataset or instructions for how to construct the dataset).
 - (d) We recognize that reproducibility may be tricky in some cases, in which case authors are welcome to describe the particular way they provide for reproducibility. In the case of closed-source models, it may be that access to the model is limited in some way (e.g., to registered users), but it should be possible for other researchers to have some path to reproducing or verifying the results.

5. Open access to data and code

Question: Does the paper provide open access to the data and code, with sufficient instructions to faithfully reproduce the main experimental results, as described in supplemental material?

Answer: [No]

Justification: We will release the code upon acceptance. All datasets used in this paper are publicly accessible.

Guidelines:

- The answer NA means that paper does not include experiments requiring code.
- Please see the NeurIPS code and data submission guidelines (<https://nips.cc/public/guides/CodeSubmissionPolicy>) for more details.
- While we encourage the release of code and data, we understand that this might not be possible, so “No” is an acceptable answer. Papers cannot be rejected simply for not including code, unless this is central to the contribution (e.g., for a new open-source benchmark).
- The instructions should contain the exact command and environment needed to run to reproduce the results. See the NeurIPS code and data submission guidelines (<https://nips.cc/public/guides/CodeSubmissionPolicy>) for more details.
- The authors should provide instructions on data access and preparation, including how to access the raw data, preprocessed data, intermediate data, and generated data, etc.
- The authors should provide scripts to reproduce all experimental results for the new proposed method and baselines. If only a subset of experiments are reproducible, they should state which ones are omitted from the script and why.
- At submission time, to preserve anonymity, the authors should release anonymized versions (if applicable).
- Providing as much information as possible in supplemental material (appended to the paper) is recommended, but including URLs to data and code is permitted.

6. Experimental setting/details

Question: Does the paper specify all the training and test details (e.g., data splits, hyperparameters, how they were chosen, type of optimizer, etc.) necessary to understand the results?

Answer: [Yes]

Justification: We provide all the experimental details in Appendix J.

Guidelines:

- The answer NA means that the paper does not include experiments.
- The experimental setting should be presented in the core of the paper to a level of detail that is necessary to appreciate the results and make sense of them.
- The full details can be provided either with the code, in appendix, or as supplemental material.

7. Experiment statistical significance

Question: Does the paper report error bars suitably and correctly defined or other appropriate information about the statistical significance of the experiments?

Answer: [Yes]

Justification: We report the standard deviation across different random seeds for all tasks.

Guidelines:

- The answer NA means that the paper does not include experiments.
- The authors should answer "Yes" if the results are accompanied by error bars, confidence intervals, or statistical significance tests, at least for the experiments that support the main claims of the paper.
- The factors of variability that the error bars are capturing should be clearly stated (for example, train/test split, initialization, random drawing of some parameter, or overall run with given experimental conditions).
- The method for calculating the error bars should be explained (closed form formula, call to a library function, bootstrap, etc.)
- The assumptions made should be given (e.g., Normally distributed errors).
- It should be clear whether the error bar is the standard deviation or the standard error of the mean.
- It is OK to report 1-sigma error bars, but one should state it. The authors should preferably report a 2-sigma error bar than state that they have a 96% CI, if the hypothesis of Normality of errors is not verified.
- For asymmetric distributions, the authors should be careful not to show in tables or figures symmetric error bars that would yield results that are out of range (e.g. negative error rates).
- If error bars are reported in tables or plots, The authors should explain in the text how they were calculated and reference the corresponding figures or tables in the text.

8. Experiments compute resources

Question: For each experiment, does the paper provide sufficient information on the computer resources (type of compute workers, memory, time of execution) needed to reproduce the experiments?

Answer: [Yes]

Justification: All the computing infrastructure information has been provided Appendix J.

Guidelines:

- The answer NA means that the paper does not include experiments.
- The paper should indicate the type of compute workers CPU or GPU, internal cluster, or cloud provider, including relevant memory and storage.
- The paper should provide the amount of compute required for each of the individual experimental runs as well as estimate the total compute.
- The paper should disclose whether the full research project required more compute than the experiments reported in the paper (e.g., preliminary or failed experiments that didn't make it into the paper).

9. Code of ethics

Question: Does the research conducted in the paper conform, in every respect, with the NeurIPS Code of Ethics <https://neurips.cc/public/EthicsGuidelines?>

Answer: [Yes]

Justification: We conform with the NeurIPS code of Ethics.

Guidelines:

- The answer NA means that the authors have not reviewed the NeurIPS Code of Ethics.

- If the authors answer No, they should explain the special circumstances that require a deviation from the Code of Ethics.
- The authors should make sure to preserve anonymity (e.g., if there is a special consideration due to laws or regulations in their jurisdiction).

10. **Broader impacts**

Question: Does the paper discuss both potential positive societal impacts and negative societal impacts of the work performed?

Answer: [Yes]

Justification: We have discussed both potential positive societal impacts and negative societal impacts in Appendix A.

Guidelines:

- The answer NA means that there is no societal impact of the work performed.
- If the authors answer NA or No, they should explain why their work has no societal impact or why the paper does not address societal impact.
- Examples of negative societal impacts include potential malicious or unintended uses (e.g., disinformation, generating fake profiles, surveillance), fairness considerations (e.g., deployment of technologies that could make decisions that unfairly impact specific groups), privacy considerations, and security considerations.
- The conference expects that many papers will be foundational research and not tied to particular applications, let alone deployments. However, if there is a direct path to any negative applications, the authors should point it out. For example, it is legitimate to point out that an improvement in the quality of generative models could be used to generate deepfakes for disinformation. On the other hand, it is not needed to point out that a generic algorithm for optimizing neural networks could enable people to train models that generate Deepfakes faster.
- The authors should consider possible harms that could arise when the technology is being used as intended and functioning correctly, harms that could arise when the technology is being used as intended but gives incorrect results, and harms following from (intentional or unintentional) misuse of the technology.
- If there are negative societal impacts, the authors could also discuss possible mitigation strategies (e.g., gated release of models, providing defenses in addition to attacks, mechanisms for monitoring misuse, mechanisms to monitor how a system learns from feedback over time, improving the efficiency and accessibility of ML).

11. **Safeguards**

Question: Does the paper describe safeguards that have been put in place for responsible release of data or models that have a high risk for misuse (e.g., pretrained language models, image generators, or scraped datasets)?

Answer: [NA]

Justification: This paper poses no such risks.

Guidelines:

- The answer NA means that the paper poses no such risks.
- Released models that have a high risk for misuse or dual-use should be released with necessary safeguards to allow for controlled use of the model, for example by requiring that users adhere to usage guidelines or restrictions to access the model or implementing safety filters.
- Datasets that have been scraped from the Internet could pose safety risks. The authors should describe how they avoided releasing unsafe images.
- We recognize that providing effective safeguards is challenging, and many papers do not require this, but we encourage authors to take this into account and make a best faith effort.

12. **Licenses for existing assets**

Question: Are the creators or original owners of assets (e.g., code, data, models), used in the paper, properly credited and are the license and terms of use explicitly mentioned and properly respected?

Answer: [Yes]

Justification: We have cited all code, data, and models we used in the paper.

Guidelines:

- The answer NA means that the paper does not use existing assets.
- The authors should cite the original paper that produced the code package or dataset.
- The authors should state which version of the asset is used and, if possible, include a URL.
- The name of the license (e.g., CC-BY 4.0) should be included for each asset.
- For scraped data from a particular source (e.g., website), the copyright and terms of service of that source should be provided.
- If assets are released, the license, copyright information, and terms of use in the package should be provided. For popular datasets, paperswithcode.com/datasets has curated licenses for some datasets. Their licensing guide can help determine the license of a dataset.
- For existing datasets that are re-packaged, both the original license and the license of the derived asset (if it has changed) should be provided.
- If this information is not available online, the authors are encouraged to reach out to the asset's creators.

13. **New assets**

Question: Are new assets introduced in the paper well documented and is the documentation provided alongside the assets?

Answer: [NA]

Justification: This paper does not release new assets.

Guidelines:

- The answer NA means that the paper does not release new assets.
- Researchers should communicate the details of the dataset/code/model as part of their submissions via structured templates. This includes details about training, license, limitations, etc.
- The paper should discuss whether and how consent was obtained from people whose asset is used.
- At submission time, remember to anonymize your assets (if applicable). You can either create an anonymized URL or include an anonymized zip file.

14. **Crowdsourcing and research with human subjects**

Question: For crowdsourcing experiments and research with human subjects, does the paper include the full text of instructions given to participants and screenshots, if applicable, as well as details about compensation (if any)?

Answer: [NA]

Justification: This paper does not involve crowdsourcing nor research with human subjects.

Guidelines:

- The answer NA means that the paper does not involve crowdsourcing nor research with human subjects.
- Including this information in the supplemental material is fine, but if the main contribution of the paper involves human subjects, then as much detail as possible should be included in the main paper.
- According to the NeurIPS Code of Ethics, workers involved in data collection, curation, or other labor should be paid at least the minimum wage in the country of the data collector.

15. **Institutional review board (IRB) approvals or equivalent for research with human subjects**

Question: Does the paper describe potential risks incurred by study participants, whether such risks were disclosed to the subjects, and whether Institutional Review Board (IRB) approvals (or an equivalent approval/review based on the requirements of your country or institution) were obtained?

Answer: [NA]

Justification: This paper does not involve crowdsourcing nor research with human subjects.

Guidelines:

- The answer NA means that the paper does not involve crowdsourcing nor research with human subjects.
- Depending on the country in which research is conducted, IRB approval (or equivalent) may be required for any human subjects research. If you obtained IRB approval, you should clearly state this in the paper.
- We recognize that the procedures for this may vary significantly between institutions and locations, and we expect authors to adhere to the NeurIPS Code of Ethics and the guidelines for their institution.
- For initial submissions, do not include any information that would break anonymity (if applicable), such as the institution conducting the review.

16. **Declaration of LLM usage**

Question: Does the paper describe the usage of LLMs if it is an important, original, or non-standard component of the core methods in this research? Note that if the LLM is used only for writing, editing, or formatting purposes and does not impact the core methodology, scientific rigorousness, or originality of the research, declaration is not required.

Answer: [NA]

Justification: We did not use LLMs.

Guidelines:

- The answer NA means that the core method development in this research does not involve LLMs as any important, original, or non-standard components.
- Please refer to our LLM policy (<https://neurips.cc/Conferences/2025/LLM>) for what should or should not be described.